Published journal article available at: https://doi.org/10.1016/j.cattod.2014.01.016

Elsevier Editorial System(tm) for Catalysis Today
Manuscript Draft

Manuscript Number: CATTOD-D-13-00449R3

Title: Electrochemical synthesis of fuels by CO2 hydrogenation on Cu in a potassium ion conducting membrane reactor at bench scale

Article Type: SI: ICCMR 2013

Keywords: Electrochemical synthesis; Bench scale; CO2 hydrogenation; Cu/K-βAl2O3; CO2 recycling

Corresponding Author: Dr. Esperanza Ruiz Martínez, Ph.D.

Corresponding Author's Institution: CIEMAT

First Author: Esperanza Ruiz Martínez, Ph.D.

Order of Authors: Esperanza Ruiz Martínez, Ph.D.; Domingo Cillero Carrera, B.S.; Pedro Juan Martínez Román, B. S.; Ángel Morales Sabio, Ph. D.; Gema San Vicente Domingo, Ph. D.; Gonzalo de Diego Velasco, Ph. D.; Jose María Sánchez Hervás, Ph. D.

Abstract: The electrochemical synthesis of fuels by CO2 hydrogenation was studied over a cheap, widespread and non-precious Cu catalyst in a potassium ion conducting membrane (K-βAl2O3) reactor at bench scale, under atmospheric pressure, at relatively low temperatures and high gas flow rates, with varying H2/CO2 ratios and using gas compositions representative of postcombustion CO2 capture exit streams and easily scalable catalyst-electrode configurations, as an approach towards its potential practical application.
The Cu catalyst film was deposited by electroless and characterised both as prepared and after testing. The presence of Cu+ and relatively big Cu particles probably determined the high selectivity to CH3OH and the unusual small selectivity to CO and CH4.
Selectivities to CH3OH, C2H5OH and C2H6O were electrochemically enhanced up to a maximum of 34, 22 and 3.4 times, respectively. The optimum temperature for the electrochemically assisted CO2 hydrogenation was selected to be 325 ºC. Higher gas flow rates favoured the synthesis of dimethyl ether at the expense of methanol and ethanol formation. CO2 conversion increased with H2/CO2 ratio, whereas selectivity to fuels showed a maximum for a H2/CO2 ratio of 2. Selectivity to dimethyl ether follows an opposite trend vs. H2/CO2 ratio with respect to methanol and ethanol ones.

Reviewer 2

Comment:
The manuscript has thoroughly revised and most of the recommendations have taken into account. However, before final acceptance authors should revise the references in the Introduction part. There are a couple of EPOC studies on CO_2 hydrogenation which have recently published and must be cited.
Answer:
As required by Reviewer 2, the references in the Introduction part of the manuscript have been revised and updated accordingly.

Reviewer 3

Comment:
1. The Authors carried out an important work to improve their paper.Answers can now be found to the main questions and major points were assessed. My opinion is that this work may now be published in Catalysis Today.
Answer:
No action/answer required.

Reviewer 4

Comment:
1. The first version of this article has a lot of problems however the revised version is improved. I suggest the publication of this work only after minor revision regarding the explanation of the conversion of the CO_2 increase as the flow rate is increased (which indicates that the results are limited by mass transfer). The alternative explanation that suggest is wrong and must be removed.
Answer:
As required by reviewer 4, the alternative explanation suggested for the increase of CO_2 conversion with gas flow rate has been removed from the manuscript. A comment on the fact that the increase in CO_2 conversion on increasing gas flow rate could be indicative of the existence of mass transfer limitations has been included in page 27 of the revised manuscript.

CATALYSIS TODAY

INVITATION LETTER

Guest Editors Name: José Sousa, Angelo Basile, João Crespo

Special Issue Title: Catalysis in Membrane Reactors. Proceedings of the 11th International Conference on Catalysis in Membrane Reactors. Porto, Portugal, 7th – 11th July 2013.

Dear Dr Esperanza Ruiz,

On behalf of the ICCMR11 Scientific Committee, we have the pleasure to invite you to submit a manuscript for the ICCMR11 Special Issue in Catalysis Today, based on your work "*Electrochemical synthesis of fuels by CO_2 hydrogenation on Cu in a potassium ion conducting membrane reactor at bench scale*".

With our Kindest Regards,

José Sousa
Angelo Basile
João Crespo

Highlights

- Electroassisted CO_2 hydrogenation on Cu/K-βAl_2O_3 under realistic conditions.
- Enhancement on CO_2 conversion and selectivity to fuels by pumping K to Cu.
- Selectivity to C_2H_6O rose and to CH_3OH and C_2H_5OH decreased with flow rate.
- CO_2 conversion increased with H_2/CO_2 ratio and gas flow rate.
- Selectivities to CH_3OH, C_2H_5OH and C_2H_6O showed a maximum for H_2/CO_2=2.

*Graphical Abstract (for review)

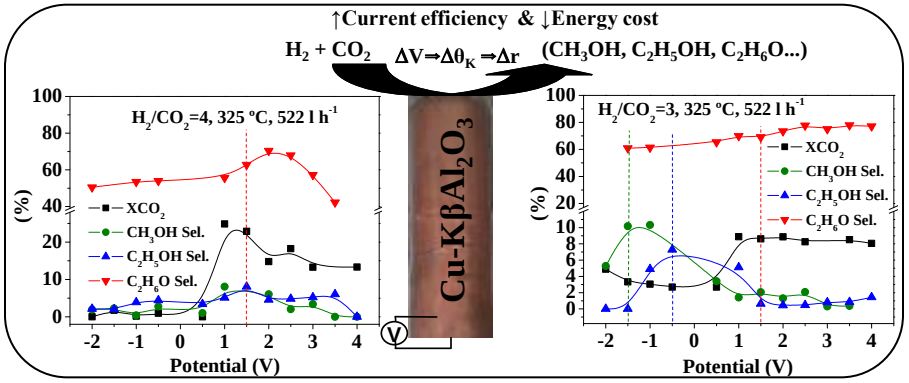

Electrochemical synthesis of fuels by CO_2 hydrogenation on Cu in a potassium ion conducting membrane reactor at bench scale

Esperanza Ruiz *, Domingo Cillero, Pedro J. Martínez, Ángel Morales, Gema San Vicente, Gonzalo de Diego, José María Sánchez

Centro de Investigaciones Energéticas, Medioambientales y Tecnológicas (CIEMAT), Av. Complutense, 40, 28040 Madrid, Spain

*Corresponding author: Tel.:+34-91-346-0887; fax.:+34-91-346-6269.

E-mail address: esperanza.ruiz@ciemat.es

Abstract

The electrochemical synthesis of fuels by CO_2 hydrogenation was studied over a cheap, widespread and non-precious Cu catalyst in a potassium ion conducting membrane (K-βAl_2O_3) reactor at bench scale, under atmospheric pressure, at relatively low temperatures and high gas flow rates, with varying H_2/CO_2 ratios and using gas compositions representative of postcombustion CO_2 capture exit streams and easily scalable catalyst-electrode configurations, as an approach towards its potential practical application.

The Cu catalyst film was deposited by electroless and characterised both as prepared and after testing. The presence of Cu+ and relatively big Cu particles probably determined the high selectivity to CH_3OH and the unusual small selectivity to CO and CH_4.

Selectivities to CH_3OH, C_2H_5OH and C_2H_6O were electrochemically enhanced up to a maximum of 34, 22 and 3.4 times, respectively. The optimum temperature for the electrochemically assisted CO_2 hydrogenation was selected to be 325 ºC. Higher gas flow rates favoured the synthesis of dimethyl ether at the expense of methanol and ethanol formation. CO_2 conversion increased with H_2/CO_2 ratio, whereas selectivity to fuels showed a maximum for a H_2/CO_2 ratio of 2. Selectivity to dimethyl ether follows an opposite trend vs. H_2/CO_2 ratio with respect to methanol and ethanol ones.

Keywords: Electrochemical synthesis, Bench scale, CO_2 hydrogenation, Cu/K-βAl_2O_3, CO_2 recycling.

1. Introduction

Due to the depletion of fossil fuels and the increasing CO_2 atmospheric levels incoming from combustion, valorisation of CO_2 to fuels is viewed as a complementary strategy for reducing CO_2 emissions, allowing their recycling and, therefore, a more sustainable use of the energy resources. Chemical recycling of carbon dioxide, as an energy carrier, from combustion sources can be achieved via its capture and subsequent hydrogenation to fuels (methanol, dimethyl ether, ethanol, etc.), given that any available renewable energy source (wind, solar or hydraulic) is used for both production of needed hydrogen (by water electrolysis) and chemical conversion of CO_2. In this way, carbon dioxide can be transformed from a detrimental greenhouse gas causing global warning into a valuable, renewable, environmentally neutral and inexhaustible fuel source for the future [1–4].

It can be predicted that increasing amounts of cheap CO_2 will be available from carbon sequestration in the near future. Moreover, the potential use of methanol and derivatives (dimethyl ether) as fuels leads to forecast a growth in the demand of both compounds. Currently, methanol is produced at industrial level from syngas streams over Cu based conventional catalysts operating at high pressure to promote the hydrogenation reaction. However, these catalysts are no so effective for CO_2-rich sources (CO_2 capture streams) under operating conditions of interest. Dimethyl ether and other hydrocarbons can be also formed over Cu based catalysts with improved CO_2 conversion [5].

The application of small currents or potentials between a metal catalyst which is in contact with a solid electrolyte and a counter electrode results in the moving of promoting species to the catalyst surface, allowing altering the catalytic performance for the CO_2 hydrogenation reaction and the selectivity to the desired products, as well as to simultaneously monitor and control the reaction during the process [6]. CO_2 hydrogenation over Cu is susceptible of being

electrochemically assisted, allowing operation of the catalyst under milder conditions [7]. The electrochemically promoted CO_2 hydrogenation reaction has been studied over Pt on YSZ (an O^{2-} conductor) [8, 9] or K-βAl_2O_3 (a K+ conductor) [10], Pd on YSZ or Na-βAl_2O_3 (a Na^+ conductor) [11], Rh on YSZ [8, 12], Ru on YSZ or Na-βAl_2O_3 [13, 14] and Ni or Ru impregnated carbon nanofibers on YSZ [15]. However, there are few previous studies of CO_2 hydrogenation over Cu in solid electrolyte ion conducting membrane reactors. It has been studied over Cu on $SrZr_{0.9}Y_{0.1}O_{3-\alpha}$ (a proton conductor) [7] and over Cu on TiO_2-YSZ [8]. In addition, these studies have been carried out using reaction conditions and gas compositions that are not representative of real postcombustion CO_2 capture exit streams. Therefore, aspects regarding the practical application of the technology have not been addressed in detail [16–18]. On the other hand, some previous works [19–23] demonstrated that CO_2 and H_2 chemisorption over Cu surfaces can be modified by the presence of potassium, and consequently the catalytic performance of Cu catalyst towards the CO_2 hydrogenation reaction can be electrochemically altered by controlling the potassium surface concentration on the catalyst surface.

This work presents a bench-scale study of electrochemical synthesis of renewable fuels by CO_2 hydrogenation over a cheap, widespread and non-precious Cu catalyst on K-βAl_2O_3, at high flow rates, under atmospheric pressure and at relatively low temperatures, using gas compositions representative of postcombustion CO_2 capture streams and catalyst-electrode tubular configurations easily adaptable to existing catalytic devices (conventional flow reactors) and prepared by a readily scalable procedure. Moreover, in this study, we evaluate the influence of temperature and gas flow rate on the extent of the electrochemically assisted CO_2 hydrogenation reaction and on the selectivity for the different target oxygenated fuels. Changing H_2/CO_2 ratios (from 2 to 4) have been explored in order to consider the effect of a discontinuous H_2 flow, as the H_2 needed for CO_2 hydrogenation may be discontinuously

produced by water electrolysis only when electricity demand is low and from intermittent renewable energy sources [2, 3].

2. Experimental

2.1 Electrochemical catalyst

The electrochemical cell evaluated in this work consisted of a thin Cu film (catalyst-working electrode) deposited by electroless on the outer surface of a 28-mm-i.d., 100-mm-long, and 1-2 mm-thick K-βAl_2O_3 tube, closed flat at one end (IONOTEC). A gold counter electrode was painted on the inner side of the solid electrolyte tube to perform polarizations. Gold was chosen as counter electrode material because it is reported [8] to be inert for the CO_2 hydrogenation reaction.

The Au counter electrode was prepared by painting the inner side of the K-βAl_2O_3 tube with a gold paste (HERAEUS-C5729). The deposited paste was dried at 150 ºC during 10 min, heated to 850 ºC at a controlled rate and, finally, annealed at 850 º C [11] during 10 min, following instructions of the gold paste supplier and taking into account recommendations given by the solid electrolyte supplier (IONOTEC).

After that, the copper layer was deposited on the outer surface of the K-βAl_2O_3 tube by electroless deposition technique. Electroless deposition [24–28] is the process of depositing a metallic coating from a solution without the application of external electrical power, so it is therefore applicable to non-conducting substrates, as is the case. Substrates need to be activated with a catalyst, usually palladium, to start deposition. Most metals, including Cu, are electrocalatytic so, once deposition starts, it keeps on going increasing layer thickness.

In this case, the outer surface of the candle was firstly cleaned with a mix of acetone and methanol (50/50) and then activated by introducing it in a solution containing 0,001M of palladium chloride followed by rinsing. After palladium activation, the K-βAl_2O_3 tube was immersed, during one hour, in the electroless deposition bath that contains: copper sulphate as metal source, sodium and potassium tartrate as complexing agent, sodium hydroxide to adjust pH and formaldehyde as reducing agent. Solution temperature was kept at 25ºC under bubbling of a small amount of air in the solution. Finally, the substrate tube was rinsed with distilled water and dried in air in an oven at 70ºC.

2.2 Catalyst characterisation

The Cu film was characterized, both as prepared and after reduction and testing, by Scanning Electron Microscopy (SEM), X-Ray Diffraction (XRD) and X-ray Photoelectron Spectroscopy (XPS) techniques.

The morphology of the catalyst film was investigated via SEM using a HITACHI S-2500 instrument of 25 kV of accelerating voltage and 35 Å of resolution.

XRD patterns of the catalyst-working electrode film were recorded on a PHILIPS "Xpert-MPD" instrument using a Cu Kα X-ray source (45 kV and 40 mA), a 2θ range of 15-75º, a step size of 2θ=0.03º and a step time of 2 s.

The surface chemical composition of the Cu film was examined by XPS using a Perkin-Elmer PHI 5400 System equipped with a Mg Kα (hν = 1253.6 eV) excitation source running at 15 kV and 20 mA and having a beam diameter of 1 mm. Base pressure in the analysis chamber was maintained at about 10^{-9} Torr. The pass energy was set at 89.5 eV for general spectra (0-1100 eV) and at 35.75 eV for high resolution spectra. The energy scale was referenced to the carbon 1s signal at 285.0 eV.

2.3 Experimental set-up

Electrochemically assisted CO_2 hydrogenation over Cu was studied in a bench-scale plant described in detail elsewhere [10].

Post-combustion CO_2 capture gas components and hydrogen can be fed by mass flow controllers. Steam can be added by vaporising water fed into a boiler by a metering pump. The mixed wet gas can be then preheated and sent to a fixed-bed down-flow quartz reactor, with 35 mm of diameter and 900 mm of length, heated by a three-zone electrical furnace. Polarization across the cell was imposed and measured using a potentiostat-galvanostat.

Gaseous products from the reactor were passed through a heated transfer line to the gas analysis system to prevent condensation of any volatile products. Gas composition was simultaneously determined using a gas microchromatograph (VARIAN CP-4900) and an NDIR CO_2/CO (FUJI ELECTRIC ZKJ) on line analyser [10], enabling the analysis of: H_2, N_2, CO, CH_4, CO_2, C_2H_2, C_2H_4, C_2H_6, C_3H_6, C_3H_8, methanol, dimethyl ether, ethanol, formic acid and acetic acid.

The gas micro-chromatograph (VARIAN CP-4900) is equipped with three column modules: a PLOT Molecular Sieve 5Å (10 m x 0.32 mm), a PORAPLOT Q (10 m x 0.15 mm) and a CP-SIL 5 CB (6 m x 0.15 mm) [10]. Each column is connected to the corresponding micro thermal conductivity detector (micro-TCD). The gas chromatography analysis was performed at constant temperature and pressure, but the conditions differ for each column module and are as follows: 40 ºC and 20 psi, 41 ºC and 25 psi and 41 ºC and 7.3 psi for the PLOT Molecular Sieve, PORAPLOT Q and CP-SIL 5 CB, respectively.

Helium is used both as carrier and reference gas for the thermal conductivity detectors.

2.4 Operating conditions and procedure

The electrochemical catalyst was appropriately placed in the reactor, with the closed flat end of the tube facing the inlet gas stream, in order to avoid by-pass phenomena and to ensure a god catalyst-reactive gas contact.

The electrical connections in the reactor were made from gold wires [8]. Both catalyst (Cu) and counter (Au) electrodes were connected via gold wires (one point-spot connection) to the galvanostat-potenciostat without using a current collector grid. The current uniformity over the entire catalyst surface was ensured because the in-plane or surface resistance of the Cu film (both as prepared and after testing) was determined to be below 1 Ohm, which is small enough (bellow 30 Ohm) [15] as to guarantee equal current distribution over the entire catalyst surface. For this purpose, after preparation of the Cu catalyst electrode and before performing any CO_2 hydrogenation tests, the in-plane or surface resistance of the Cu catalyst film was obtained by measurement of the electric resistance between two point contacts taken at different distance from each other (from 10 mm to 90 mm). In the case of Au counter electrode film the corresponding surface resistance resulted to be also very low (of about 0.4 Ohm).

Before the CO_2 hydrogenation tests, the Cu film was firstly reduced in a stream of H_2 at 400 ºC during 1 h [10].

A positive potential of 4 V was applied between the Cu and the Au electrodes during 30 min prior to each test in order to clean the Cu catalyst surface from potassium ions, which could thermally migrate to the catalyst surface, and to ensure the decomposition of any potential carbon dioxide adsorbed species, as a way to define a reproducible reference state (unpromoted state) of the Cu catalyst surface. At the end of this time, the current density dropped to almost zero. This potential value is about the decomposition voltage, i.e., the

electrode potential above which the current starts to increase appreciably concurring with solid electrolyte decomposition, reported for Na-βAl_2O_3 [29]. However, in accordance with literature [30], no evidence of solid electrolyte decomposition could be found from the dependence of current on potential observed in previous cyclic voltammetry studies of the Cu catalyst (not shown). The stability of the K-βAl_2O_3 electrolyte was confirmed by measurements of the cell resistance before and after hydrogenation tests, which revealed that it stayed the same after testing.

The electrochemical experiments were performed both under temperature programmed manner, by following the effect of temperature (between 200 to 400 ºC) on the catalytic performance and selectivity at different applied potentials, and under potentiostatic mode, by following the influence of the applied potential (between 4 and -2 V) on CO_2 conversion and selectivity to the different products at a given temperature. The effect of polarization (under application of constant potentials from 4 to -2 V) on catalyst performance was investigated at the temperature selected from the temperature programmed tests, using different gas flow rates (90 and 522 l h^{-1}) and H_2/CO_2 ratios (between 2 and 4) to determine the influence of operating conditions on CO_2 conversion and selectivity to the different products.

CO_2 hydrogenation tests were performed under H_2 and CO_2 binary mixtures, although a small amount of N_2 (about 0.5 %) was added to the reaction gas mix as an internal standard. Accordingly [10], CO_2 conversion (X_{CO_2}) and "CO_2 free selectivity" is defined as (1) and (2), respectively:

$$X_{CO_2} = \left(1 - \frac{[CO_2]_o \times [N_2]_i}{[CO_2]_i \times [N_2]_o}\right) \times 100 \quad (1)$$

$$Si = \frac{n_i \times M_i}{\sum_{i=1}^{i=n} n_i \times M_i} \times 100 \quad (2)$$

Where $[CO_2]_i$ and $[CO_2]_o$ are the corresponding CO_2 molar quantities at the inlet and outlet of the reactor. As well, $[N_2]_i$ and $[N_2]_o$ are N_2 molar quantities at the inlet and outlet of the reactor, respectively. Additionally, S_i is the selectivity to product i, n_i is the number of carbon atoms of product i and M_i is moles of product i, respectively.

The coverage of potassium (Θ_K) established on the Cu surface for each applied potential at steady state conditions was estimated according to Faraday`s law (3) [31]. Where F is the Faraday's constant, N is the surface mol or electrochemical active surface area (mol of active sites) of the Cu catalyst electrode, I is the current observed upon application of each potential (V) and t is time of current application (1500 s at each potential).

$$\theta_K = (-I \times t)/(F \times N) \quad (3)$$

The effect of polarization on catalyst performance for the CO_2 hydrogenation reaction was gauged in terms of promotion index (PI_{Ki}) (4) [6] for each fuel product formation (methanol, ethanol and dimethyl ether).

$$PI_{Ki} = \frac{\Delta r_i / r_{oi}}{\theta_K} \quad (4)$$

Where Δr_i, is the electropromoted variation in catalytic rate of formation of product i and r_{oi}, is the unpromoted catalytic rate of formation of product i.

The value of current efficiency or Faradaic efficiency (η_c) and energy cost (C_E) were calculated for each fuel product formation (methanol, ethanol and dimethyl ether) under different applied potentials and operating conditions, following the expressions (5) and (6), respectively:

$$\eta_c = \left\{(m_p / M_p) \times \nu_e / \nu_p \times F\right\}/(I \times t) \quad (5)$$

$$C_E = V \times F \times (\nu_e / \nu_p)/(\eta_c \times M_p) \quad (6)$$

Where, ν_e is the number of electrons transferred and ν_p is the stoichiometric coefficient in each product formation reaction. Additionally, m_p and M_p are the mass and molecular weight of product formed, respectively.

3. Results and Discussion

3.1 Catalyst characterisation studies

As reported in literature [6], the utilised preparation technique determines also porous structure, surface morphology and particle size of the metal thin film and therefore the electrochemically assisted catalytic behaviour of the system.

SEM micrographs of Cu catalyst-working electrode film, both as prepared and after testing, are shown in Fig. 1a and Fig. 1b, respectively. XRD patterns of the Cu catalyst-working electrode film, both as prepared and after testing, are also depicted in Fig. 2a and Fig. 2b, respectively. The peak at around 2θ=43.3 was identified as the main diffraction peak of metallic Cu (JCPDS card no. 01-085-1326); whereas the peak at about 2θ=36.5 was assigned to the main diffraction peak of Cu_2O (JCPDS card no. 01-077-0199). The rest of the peaks may be ascribed to the K-βAl_2O_3 solid electrolyte (JCPDS card no. 00-051-0769 and 01-084-0380).

Moreover, the average crystallite size of the samples was evaluated from X-ray broadening of the main metallic Cu diffraction peak at 2θ = 43.3 by using the well-known Debey-Scherrer equation [32, 33]. The average particle size resulted to be of about 23 nm for the fresh catalyst and around 60 nm for the used sample.

As can be observed in Fig. 1a, the obtained Cu film seems to resemble a typical foam structure [34], suggesting that it is porous (allowing reactants and products diffusion), with a

small particle size (associated with high reactivity), as determined by XRD, and continuous, as verified by electrical conductivity measurements. Therefore, the utilised electroless technique allows preparation of a thin Cu catalyst film with the suitable morphology, microstructure and electrical properties (surface resistance below 1 Ohm) required for the electrochemically assisted tests [35]. XPS analysis results (not shown) confirmed also that the Cu catalyst surface (as prepared) was free of chlorine or any other poisoning adsorbent which could be potentially incorporated in the course of catalyst preparation by electroless.

It seems that exposure of the Cu catalyst film to hydrogen and reducing testing gas environment resulted in an almost complete reduction of Cu oxide to metallic Cu and in sintering of metallic Cu particles [36], giving rise to an increase in Cu particle size, as resembled by the fact that reference XRD peak of Cu_2O almost disappeared and metallic Cu XRD peak turned sharper in the used sample.

Cu metal dispersion has been also estimated from the obtained particle diameter [37]. Cu dispersion decreases from 4.7 % in the fresh sample to 1.8 % in the used sample. In addition, the surface Cu/Al ratios obtained from XPS technique, which reflect the copper dispersion on alumina support [38], were found to be 3.5 and 2.4 for fresh and used samples, respectively. Therefore, as reported by literature [36, 39], after reduction and reaction, metallic Cu crystallites sinter increasing their size while decreasing Cu dispersion.

In fact, according to XRD analysis, there is a redox between metallic Cu (Cu^o) and Cu_2O (Cu^+) involved in the mechanism of Cu catalysis. Two models [40, 41], redox and formate decomposition/hydrogenation pathways, have been proposed to explain the mechanism of CO_2 hydrogenation on Cu-based catalysts. In the redox model, CO_2 dissociation takes place on Cu^o to form CO (which could be further hydrogenated to other products) and Cu_2O which is subsequently reduced by hydrogen. CO_2 dissociation may be inhibited in the case of Cu_2O was not completely reduced by hydrogen, therefore a parallel pathway was suggested, the formate

decomposition/hydrogenation mechanism, in this case, the intermediate is proposed to be the formate species produced from association of hydrogen and CO_2 [40–43], which may result in methanol formation by hydrogenation and/or in CO/CO_2 release by decomposition. Cu^o and Cu+ were proposed to coexist on the Cu catalyst surface, in special in the presence of potassium [42]. The role of Cu^o is possibly to dissociate H_2 and supply atomic hydrogen required for hydrogenation reaction [40, 44, 45]. Cu^o has been also reported to enhance the rate of formate species formation and hydrogenation, whereas the presence of Cu+ (especially in small amounts) is reported to improve, apart from CO_2 adsorption, formate intermediate stability and its hydrogenation (hydrogen addition) resulting in an enhanced selectivity to methanol [40, 42, 43]. Therefore, although the Cu film was pre-reduced in H_2 before performing any tests, Cu_2O may be formed in CO_2 dissociation over metallic Cu upon exposure to H_2/CO_2 binary mixtures during testing [40–42]. In addition, as reported by literature [43], CH_3OH formation is associated with the presence of Cu+ surface species which seems to be reduced simultaneously. Moreover, the presence of potassium is reported to both stabilize copper ions under reduction and to cause the formation of Cu+ by electron withdrawing [42]. The balance between the different phenomena results in the observed catalytic performance and Cu_2O/metallic Cu distribution.

The electrochemical active surface area (mol of active sites) of the Cu catalyst-electrode film (as prepared) was calculated [15] using the estimated Cu metal dispersion value and the known Cu loading (total amount of metal deposited in moles) and resulted to be 1×10^{-4} mol Cu.

3.2 CO_2 hydrogenation tests

3.2.1 Effect of temperature

Fig. 3 shows the steady state effect of temperature on the conversion of CO_2 and on the selectivity to CH_3OH, C_2H_5OH and C_2H_6O over a clean Cu surface (+ 4 V) (Fig. 3a), without polarization (0 V) (Fig. 3c) and under anodic (+2 V) (Fig. 3b) and cathodic (-2 V) (Fig. 3d) polarization conditions, at temperatures from 200 to 400 ºC, at 90 l h^{-1} of total gas flow rate and using a H_2/CO_2 ratio of 3.

In absence of polarization (0 V), although no electrical current passes across the cell, potassium promoter ions could also thermally migrate from the solid electrolyte to the catalyst surface as temperature increases, due to the increased ionic conductivity of the solid electrolyte at higher temperatures.

The main products obtained were methanol, dimethyl ether and ethanol, but CO, CH_4, C_2+C_3 hydrocarbons, formic acid and acetic acid were also detected to be formed. CO_2 conversion shows a maximum at certain temperature for whatever the applied potential. The selectivity to CH_3OH and C_2H_6O exhibited also a maximum at a given temperature and then decreased with the temperature increment, whereas selectivity to C_2H_5OH monotonically decreases as temperature increases, which agree with the fact that the equilibrium conversion of CO_2 to methanol and ethanol decreases as temperature increases. In fact, the equilibrium conversion of CO_2 to methanol increases with the increase of pressure and decreases strongly as temperature increases [46, 47], whereas the equilibrium conversion of CO_2 to ethanol decreases with increasing temperature and decreasing pressure and the ratio of H_2/CO_2 in the reaction gas [48]. In all cases, the selectivity to C_2H_5OH or C_2H_6O is higher when selectivity to CH_3OH is lower. This seems to indicate that formation of CH_3OH, C_2H_5OH and C_2H_6O are in competition over the Cu catalyst surface. A H_2/CO_2 ratio of 3 matched with the theoretical stoichiometry in the methanol, ethanol and dimethyl ether synthesis reactions by CO_2 hydrogenation according to equations (7) to (9), and thus they are thermodynamically favoured under these conditions.

$$CO_2 + 3H_2 \rightarrow CH_3OH + H_2O \quad (7)$$

$$2CO_2 + 6H_2 \rightarrow C_2H_5OH + 3H_2O \quad (8)$$

$$2CO_2 + 6H_2 \rightarrow C_2H_6O + 3H_2O \quad (9)$$

Moreover, C_2H_5OH and C_2H_6O can be also formed by hydrogenation (10)/hydration (11) and dehydration (12) of CH_3OH, respectively.

$$2CH_3OH + 3H_2 \rightarrow C_2H_5OH + H_2O \quad (10)$$

$$2CH_3OH + H_2O \rightarrow C_2H_5OH \quad (11)$$

$$2CH_3OH \rightarrow C_2H_6O + H_2O \quad (12)$$

In fact, as reported by literature [46], methanol converted to dimethyl ether at 250-300 ºC and both methanol and dimethyl ether are reported to be transformed into hydrocarbons at temperatures about 400 ◦C [49], where RWGS (13) and methanation (14) reactions are also favoured [8].

$$CO_2 + H_2 \rightarrow CO + H_2O \quad (13)$$

$$CO_2 + 4H_2 \rightarrow CH_4 + 2H_2O \quad (14)$$

Fig. 4 compares CO_2 conversion (a) and selectivity to methanol (b), ethanol (c) and dimethyl ether (d) curves vs. temperature obtained for different applied potentials.

Over an electrochemically cleaned Cu surface (4 V), CO_2 conversion shows a maximum (around 3 %) at about 250 ºC. Cathodic (-2 V) polarization leads to a significant increase in CO_2 conversion which reaches about 6 % at 275 ºC. Without polarization (0 V) and under anodic (+2 V) polarization, the maximum CO_2 conversion, at low temperature (around 300 ºC) where methanol formation is favoured [46, 47], was about 1.5 % and 2.5 %, respectively.

In the absence of surface potassium (4 V), the selectivity to CH_3OH and C_2H_6O attained a maximum of about 15 % and 45 %, respectively, around 325 ºC and 275 ºC, correspondingly and then decreased with the temperature increment, whereas selectivity to C_2H_5OH

monotonically decreased from about 35 % at 200 ºC to around 10 % at 400 ºC. Decreasing the applied potential leads to a significant increase in the maximum of CH_3OH selectivity, which reaches about 45%, 40% and 20 % without polarization (0 V) and under anodic (+2 V) and cathodic (-2 V) polarizations, respectively, and it is obtained at lower temperature (around 300 ºC-325 ºC). Selectivity to C_2H_5OH is only noticeably enhanced in the absence of polarization (0V), reaching a maximum of about 25 % at around 325 ºC. At temperatures above 325 ºC, the application of both 0 V and anodic (+2 V) polarization leads to a significant increase in C_2H_6O selectivity, reaching a maximum of about 45 % and 50 %, respectively, whereas the application of cathodic (-2 V) polarization gives rise to an improvement in selectivity to C_2H_6O (up to about 40 %) at temperatures below about 250 ºC.

Results obtained at different temperatures revealed that CO_2 conversion and selectivity to the different target products were maximum at temperatures around 300-325 ºC, for any applied potential. Therefore, a temperature value of 325 ºC was selected for subsequent experiments, given that the potential promoting effect of potassium increases with temperature as a result the improved ionic conductivity of the solid electrolyte at higher temperatures.

3.2.2 Effect of potential

The steady state influence of polarization on the behaviour of the Cu electrocatalyst was investigated through potentiostatic experiments performed at two different gas flow rates (90 and 522 $l\ h^{-1}$) in order to analyse the influence of gas flow rate on CO_2 hydrogenation under the stoichiometric H_2/CO_2 ratio of 3 at the selected temperature of 325 ºC. In order to consider the less favourable, although more realistic, conditions associated with a discontinuous flow of renewable H_2 [2], the behaviour of the catalyst was also studied using

H_2/CO_2 ratios of 2 and 4, which correspond to a lack and an excess of H_2, respectively, in relation to the stoichiometry of the oxygenates (CH_3OH, C_2H_5OH and C_2H_6O) formation reactions, (7) to (9).

Fig. 5 depicts the response of CO_2 conversion and selectivity to CH_3OH, C_2H_5OH and C_2H_6O to different applied potentials (between 4 and -2 V). The experiments were carried out at 325 ºC and 90 l h^{-1} and using a H_2/CO_2 ratio of 3.

As commented above, for H_2/CO_2 ratios of 3, the hydrogenation of CO_2 over the electrocatalyst, at 325 ºC and 90 l h^{-1}, gives rise mainly to the formation of the different target oxygenates, in addition to (not shown) formic acid (15), acetic acid (16) and C_2+C_3 hydrocarbons, mostly as C_2H_6 (17) and C_3H_6 (18). CH_4 and CO were almost undetected to be formed under these conditions.

$$CO_2 + H_2 \rightarrow HCOOH \quad (15)$$

$$2\,CO_2 + 4\,H_2 \rightarrow CH_3COOH + 2\,H_2O \quad (16)$$

$$2\,CO_2 + 7\,H_2 \rightarrow C_2H_6 + 4\,H_2O \quad (17)$$

$$3\,CO_2 + 9\,H_2 \rightarrow C_3H_6 + 6\,H_2O \quad (18)$$

In this case, CO_2 hydrogenation is affected significantly by the applied potential, with selectivities to CH_3OH, C_2H_5OH and C_2H_6O up to 27.7 %, 27.9 % and 47.1 %, respectively, but CO_2 conversion is rather low The catalyst showed an electrophilic electrochemical behaviour, i.e., CO_2 conversion increases with the presence of the electrochemical promoter, due to the enhanced CO_2 adsorption, while selectivities to CH_3OH, C_2H_5OH and C_2H_6O exhibited a “volcano type” electrochemical behaviour, i.e., they reach a maximum at a certain potential or potassium surface coverage.

As can be deduced from Fig. 5, it seems that oxygenates formation is promoted around 0V, being a competition for the formation of the different hydrogenation products over the catalyst surface.

As can be observed in Fig. 5, the optimum applied potential for CH_3OH, C_2H_5OH and C_2H_6O formation is about 1 V (Θ_K= 2.02), 0.5 V (Θ_K= 2.32) and -0.5 V (Θ_K= 8.56), respectively, which corresponds with an enhancement in its selectivity of up to 6, 3 and 2 times and with a promotion index of 1.3, 0.2 and 0.13, respectively, i.e., increasing or decreasing applied potential from this value resulted in a decrease in the selectivity. Chemisorption of reactive molecules on a catalyst is the previous step to any catalytic process. Chemisorption of an adsorbate on a metal implies electron donation from metal to adsorbate or from adsorbate to metal. In the first case, the adsorbate is called electron acceptor (electronegative), whereas in the second, is called electron donor (electropositive). There is a certain scale of electronegativity or electron acceptor capacity [6]. In the K-βAl_2O_3 system, potassium ions can electrochemically migrate, via application of decreasingly potentials, from the solid electrolyte to the Cu catalyst electrode favouring the adsorption of electron acceptor molecules, like CO_2, whereas, at the same time, hindered the adsorption of electron donor species (H_2 in this case), giving rise to an increase in CO_2 (electron acceptor) coverage and to a decrease in the coverage of H_2 (electron donor) and therefore, modifying metal bond capacity which each reactive molecules and thus, its catalytic behaviour [6, 9, 13, 50].

In this way, depending on the relative electronegativity of the different adsorbates which participate in the reaction and on which of them is in excess over the catalyst surface, the application of polarization will have a positive or negative effect on the overall kinetics of the process [6, 50]. Thus, there is a given value of potential or promoter coverage which optimizes catalyst performance and selectivity to the desired product, which depends on temperature and gas composition.

Therefore, the observed electrochemically assisted catalytic behaviour can be rationalized considering the effect of varying applied potential on the chemisorptive bond strength of reactants and intermediate surface species [6, 50] and in accordance with the mechanisms

proposed for the CO_2 hydrogenation reaction over Cu [42, 51–57]. CO_2 does not chemisorb on clean Cu surfaces [19–21, 58–60]. However, the presence of K on Cu surface is reported [19–21] to promote CO_2 activation (19), resulting in the formation of a highly distorted CO_2 molecule (CO_2*-) interacting strongly with the surface [20, 21], which indicates that CO_2 is always adsorbed as an electron acceptor [6].

$$CO_2 + e \rightarrow CO_2^{*-} \text{ (ads.)} \quad (19)$$

The application of high positive potentials (electrochemically cleaned Cu surface), gives rise to a migration of potassium ions from the catalyst surface to the solid electrolyte, resulting in an increase of the catalyst work function, which favours the transfer of electrons from electron donor molecules, like H_2, to the Cu catalyst [61], and, thus, enhances the dissociative adsorption of the latter (20) on the Cu catalyst surface, giving rise to an increase in H_2 coverage and to a decrease in the coverage of CO_2, being CO_2 (electron acceptor) adsorption (19) the reaction limiting step [6–8, 61].

$$H_2 \rightarrow 2\,H^{*+} \text{ (ads.)} + 2\,e \quad (20)$$

Therefore, CO_2 hydrogenation over Cu based catalysts is initially limited by these two first steps: (19) CO_2 adsorption and (20) H_2 dissociation to create adsorbed atomic hydrogen. The third step can follow a dual pathway, which leads to hydrogenated products creation via adsorbed CO or formate intermediate species [22, 42, 51–57, 62].

Surface formate species produced from association of adsorbed CO_2 and H atoms (21) [22, 42, 52–57], can be further hydrogenated to formic acid (22) [56, 57], methanol (23) [52, 54, 55], etc.

$$CO_2^{*-} \text{ (ads.)} + H \text{ (ads.)} \rightarrow HOOC^{*} \text{ (ads.)} \quad (21)$$

$$HOOC^{*} \text{ (ads.)} + H \text{ (ads.)} \rightarrow HCOOH \quad (22)$$

$$HOOC^{*} \text{ (ads.)} + 5\,H \text{ (ads.)} \rightarrow CH_3OH + H_2O \quad (23)$$

Moreover, CO_2 dissociative adsorption on Cu is considered to be enhanced by the presence of coadsorbed hydrogen (24) [56, 57]. CO adsorbed species resulting from CO_2 dissociation or formate decomposition (25) [22, 42, 52–57] may desorb in the gas phase (26) or can gradually lead to highly hydrogenated molecules formation. In fact, according to literature [56, 57], from CO, methanol (27) and CH_2 radicals (28) can be directly produced. CH_2 radicals can react with hydrogen to form CH_4 (29) or C_2+C_3 hydrocarbons. Ethanol (30 and 31), dimethyl ether (32) and other multi-C alcohols can be also formed from adsorbed CO.

$$CO_2^{*-}\ (\text{ads.}) + e + 2\,H^+ \rightarrow CO^*\ (\text{ads.}) + H_2O \quad (24)$$

$$HOOC^*\ (\text{ads.}) + H\ (\text{ads.}) \rightarrow CO^*\ (\text{ads.}) + H_2O \quad (25)$$

$$CO^*\ (\text{ads.}) \rightarrow CO \quad (26)$$

$$CO^*\ (\text{ads.}) + 4\,H\ (\text{ads.}) \rightarrow CH_3OH \quad (27)$$

$$CO^*\ (\text{ads.}) + 4\,H\ (\text{ads.}) \rightarrow CH_2^*\ (\text{ads.}) + H_2O \quad (28)$$

$$CH_2^*\ (\text{ads.}) + 2\,H\ (\text{ads.}) \rightarrow CH_4 \quad (29)$$

$$CH_2^*\ (\text{ads.}) + CO^*\ (\text{ads.}) + 4\,H\ (\text{ads.}) \rightarrow C_2H_5OH \quad (30)$$

$$CH_3OH + CO^*\ (\text{ads.}) + 2\,H\ (\text{ads.}) \rightarrow C_2H_5OH \quad (31)$$

$$3\,CO^*\ (\text{ads.}) + 6\,H\ (\text{ads.}) \rightarrow CH_3OCH_3 + CO_2 \quad (32)$$

A H_2/CO_2 ratio of 3 is about the stoichiometric ratio required for CH_3OH, C_2H_5OH and C_2H_6O production and thus these reactions are thermodynamically favoured and are in competition over the catalyst surface under these conditions. Moreover, it can be observed that under application of decreasing positive potentials (low potassium coverage) formation of CH_3OH, C_2H_5OH and C_2H_6O is increasingly promoted reaching a maximum at about 1 V, 0.5 V and -0.5 V, respectively. Decreasing catalyst potential gives rise to the migration of potassium promoter species from the solid electrolyte to the Cu catalyst electrode, resulting in a decrease of the catalyst work function, which favours the transfer of electrons from the Cu

catalyst to electron acceptor molecules, like CO_2, and, thus, favours the adsorption of the latter on the Cu catalyst surface, whereas H_2 dissociative adsorption is hindered. The coverage of formate species are reported to increase also in the presence of potassium. In fact, it has been reported [36, 42] that new active sites are created at the interface between copper and potassium which are able to generate formate species and are active in higher alcohol synthesis. In addition, it has been reported that the presence of potassium may also favours hydrogenation of adsorbed CO species via polarization of the CO molecule [60].

CH_3OH, C_2H_6O and C_2H_5OH should be preferentially formed under conditions where surface coverage of both reactants (CO_2 and H_2) is expected to be very similar (under medium potassium coverage around 0V). CO_2 does not adsorb in clean Cu surfaces (in absence of potassium at highly positive potentials) [19–21, 58–60] and, at the same time, Cu, which has a relatively high hydrogen reaction overpotential [56], is somewhat catalytic for hydrogen evolution (at very negative potentials), therefore, a competition between CO_2 and H_2 adsorption could be expected, and, thus, according to this mechanism, it is expected that the formation of CH_3OH, C_2H_5OH and C_2H_6O will be limited by the adsorption of both H_2 and CO_2 [56, 57].

A subsequent decrease in potential, i.e., a further increase in potassium coverage, gives rise to an additional enhancement of CO_2 adsorption on Cu surface, and to a further decrease in H_2 dissociative adsorption. Moreover, surface formate species are reported to decompose (33), preferentially to H_2 and CO_2 instead to CO and H_2O, at high potassium surface coverages [42]. Therefore, a subsequent decrease in potential results in a decrease in selectivity to CH_3OH, C_2H_5OH and C_2H_6O, because both formate decomposition (33) and hydrogen evolution (34) reactions are favoured on increasing potassium surface coverage, and the amount of both adsorbed on the surface is reduced and could limit CO_2 hydrogenation reactions. In addition, as more water and CH_3OH are formed, the amount of surface CO

potentially generated by hydrogen enhanced CO_2 dissociation or formate decomposition could decrease also trough the WGS (water gas shift) (35) reaction [54], which is also promoted in the presence of potassium [61], and via blocking of RWGS (reverse water gas shift) reaction (13) active sites by CH_3OH [8], contributing also to the observed decrease in oxygenates selectivity.

$$HOOC^{*}\,(ads.) + H\,(ads.) \rightarrow CO_2 + H_2 \quad (33)$$

$$2\,H\,(ads.) \rightarrow H_2 \quad (34)$$

$$CO^{*}\,(ads.) + H_2O \rightarrow CO_2 + H_2 \quad (35)$$

The catalyst shows an electrophilic electrochemical behaviour i.e., CO_2 conversion increases on decreasing the applied potential as a result of the improved CO_2 adsorption.

As commented above, under the utilised operating conditions, CO and CH_4 were almost undetected to be formed. The electrocatalytic activity of Cu for RWGS reaction is reported to be quite low [7]. Moreover, as reported by literature [42, 62, 63], the presence of Cu+ species in the catalyst, as confirmed by XRD and XPS analysis of both fresh and used samples [42], probably determined the high selectivity to CH_3OH and the unusual small selectivity to CO and derived CH_4 [63], because RWGS is more favoured on metallic copper than on partially oxidized copper [44]. In addition, CO_2 and CO dissociation to form surface CO and CH_4 precursor species, respectively, is restricted over the relatively big Cu particles of the catalyst. In fact, as reported by literature [39], the size of copper particles significantly affects the selectivity to methanol, in special at low CO_2 conversion levels, i.e., larger particles (> 12 nm) are considerably more selective to methanol than smaller ones (< 3 nm). Moreover, CO dissociation, to form CH_4 precursor surface species, is also restricted over bigger particles [11, 64]. In addition, the potentially formed CO is able to be strongly adsorbed on Cu surfaces [44], according to the proposed mechanism [42] and, as commented above, decomposition of surface formate species induced by potassium tends to produce H_2 and CO_2 instead to form

CO and H_2O [42]. The presence of potassium is believed to decrease also the availability of hydrogen atoms required for CH_4 formation [61]. In addition, the potentially formed methanol is reported to block active sites for RWGS reaction [8], limiting also CO production.

3.2.3 Effect of gas flow rate

In order to analyse the impact of gas flow rate variation on the catalyst performance, an additional series of potentiostatic tests was carried out at 325 ºC and 522 l h^{-1} and using a H_2/CO_2 ratio of 3. Fig. 6 shows the steady state effect of applied potential variation (between 4 and -2 V) on CO_2 conversion and on the selectivity to CO, CH_3OH, C_2H_5OH and C_2H_6O under these conditions. The carbon mass balance (relative difference between carbon mass at the reactor inlet and outlet) was also calculated for each test. As an example, the values of carbon balance obtained for each applied potential are also shown in Fig. 6.

As can be observed in Fig. 6, at higher gas flowrate, the hydrogenation of CO_2 over the Cu catalyst film gives rise to CO formation in addition to oxygenated compounds, and it is, as well, perceptibly influenced by the applied potential, with selectivities to CH_3OH, C_2H_5OH, C_2H_6O and CO up to 10.3 %, 7.3 %, 78 % and 14.9 %, respectively, but CO_2 conversion is still quite low (up to 8 %) and CH_4 formation is also negligible [54]. The carbon balance was closed to below 0.4 % for all applied potentials.

The catalyst showed an electrophobic electrochemical behaviour, i.e., CO_2 conversion decreases with decreasing applied potential and thus with increasing potassium surface coverage, presumably due to the favoured formate decomposition. Selectivity to C_2H_6O and CO decreased with lowering catalyst potential showing also an electrophobic electrochemical behaviour, whereas selectivities to CH_3OH and C_2H_5OH exhibited a “volcano type”

electrochemical behaviour, i.e., they reach a maximum at certain potential or potassium coverage.

As can be extracted from Fig.6, the optimum potential for C_2H_6O formation seems to be 1.5 V, which corresponds with a minimum in potassium coverage (of about 0.09) and with a maximum in current efficiency (of about 2419.5) and promotion index (of about 36) for C_2H_6O formation, and given the simultaneous high CO_2 conversion and low selectivity to the rest of the products, which would result in higher yield of a finest C_2H_6O product.

As can be seen in Fig. 6, for higher gas flow rates (or reciprocally lower contact times) CO production is enhanced at positive potentials, while CH_3OH formation appears to be favoured at negative potentials, which seems to indicate that it is mainly produced directly from adsorbed CO_2 via the formate route according to reactions (21) and (23).

It seems that in this case, under application of high positive potentials, CO formed through hydrogen enhanced CO_2 dissociation (24) or formate decomposition (25) [42] tends to desorb (26) instead to further react over the catalyst surface, because CO is also a weaker electron donor than hydrogen and its adsorption is also hindered at high positive overpotentials, being RWGS (13) favoured under these conditions.

As can be deduced from Fig. 6, on decreasing applied potential, formation of CH_3OH and C_2H_5OH is increasingly promoted reaching a maximum, at about -1.5 V (Θ_K= 6.03) and -0.5 V (Θ_K= 8.56), which corresponds with an enhancement in its selectivity of up to 34 and 9 times and with a promotion index of 2.4 and 0.5, respectively. Decreasing catalyst potential results in the migration of potassium promoter species to the catalyst electrode, favouring CO_2 (electron acceptor) adsorption on Cu surface. Adsorbed CO_2 can be gradually hydrogenated, via formation of surface formate, to formic acid (22) and highly hydrogenated molecules [42], such as methanol (23), up to a maximum. In addition, as commented above, as more water and CH_3OH is formed, the increase in selectivity to alcohols could be also due to a

concomitant decrease in CO yield. In addition, water formed as a co-product in CO_2 hydrogenation has been reported to be instrumental in the formation of methanol from formate like species on supported Cu based catalysts [44].

A subsequent decrease in potential and, then, an additional increase in surface potassium coverage results in a decrease in selectivity to CH_3OH, C_2H_5OH and C_2H_6O, because, as commented above, the hydrogen evolution and formate decomposition reactions are favoured, and the amount of both adsorbed on the surface is reduced and could limit CO_2 hydrogenation reactions. In addition, close inspection of Fig. 6 shows that CH_3OH formation still remains at the lowest applied potential tested and that higher amount of CH_3OH is formed when the decomposition of surface formate species is supposed to begin. The decomposition of these formate species releases hydrogen to the surface which is then able to hydrogenate some undecomposed formate to form CH_3OH. Therefore, under these conditions, surface formate hydrogenation could be the rate determining step in CH_3OH synthesis [65].

In an attempt of clarifying the CH_3OH formation path from CO_2, the influence of gas flow rate (the reciprocal of contact time) on CO_2 hydrogenation behaviour is depicted in Fig. 7. Results indicate that increasing gas flowrate, and correspondingly, decreasing contact time, resulted in an increase in CO_2 conversion (Fig.7 a) and dimethyl ether selectivity (Fig. 7 d) and in a decrease in C_2H_5OH selectivity (Fig. 7 c) and in the maximum of CH_3OH selectivity (Fig. 7 b) which is, in addition, shifted to lower potentials (from 1 V to -1.5 V).

According to literature [54], the mechanism of CH_3OH formation changes depending on the utilised contact time range. At low contact times, which correspond with high gas flow rates, CH_3OH is mainly produced directly from CO_2, via adsorbed formate species, according to reaction (23) and CO is formed via the parallel RWGS reaction, whereas for high contact times (or low gas flow rates), another contribution to CH_3OH should be considered, that is

CH_3OH is formed from adsorbed CO deposited by the hydrogen enhanced CO_2 dissociation according to equation (27).

It can be also extracted from Fig. 7b that at high gas flow rates, i.e., at low contact times, where the formate route seems to be dominant, methanol formation is promoted at negative potentials or high potassium surface coverage, whereas for low gas flow rates (high contact times), methanol formation is promoted at positive potential or low potassium surface coverages, where methanol appears to be predominantly produced via the RWGS route.

Selectivity to methanol (at positive potentials) and ethanol decreased on increasing gas flow rate [66, 67]. On the contrary, selectivity to C_2H_6O increases on increasing gas flow rate. This could be indicative of the fact that C_2H_6O and CH_3OH are produced in parallel paths through the corresponding direct hydrogenation reactions, because a diminution in selectivity to C_2H_6O with the increase in gas flow rate could be expected if C_2H_6O was produced via consecutive dehydration of the formed CH_3OH [36, 49]. However, C_2H_5OH selectivity decreases with the increment in gas flow rate as CH_3OH does, which seems to indicate that C_2H_5OH is formed in any consecutive reaction from CH_3OH or from the same reaction intermediate.

According to literature [67], the observed decrease in C_2H_6O selectivity at higher residence times (especially at positive potentials) could resemble a possible inhibition of primary dimethyl ether synthesis, via hydrogenation of the adsorbed CO deposited by the hydrogen enhanced CO_2 dissociation (RWGS route), by H_2O formed as side product of higher alcohols and by hydrocarbons secondary reactions of adsorbed CO with CH_2^* radicals, which are favoured by long residence times.

In view of these results, it seems that the increase in gas flow rate favours the synthesis of dimethyl ether at the expense of methanol and ethanol ones.

However, given that, as commented above, CO_2 conversion increases with flow rate increase (especially at positive potentials), the presence of mass transfer limitation phenomena could not be ruled out [8].

In addition, on increasing gas flow rate, the electrochemical behaviour of the catalyst for the CO_2 hydrogenation reaction shifts from electrophilic to electrophobic, in accordance with the change in the main reaction pathway and with the variation in the adsorbed amount of the corresponding reaction intermediate with potassium surface coverage.

3.2.4 Effect of H_2/CO_2 ratio

The effect of H_2/CO_2 ratio on catalyst performance was investigated through potentiostatic experiments performed at two additional H_2/CO_2 ratios (2 and 4) at 325 ºC and 522 l h^{-1}.

The steady state response of CO_2 conversion and selectivity to CH_3OH, C_2H_5OH and C_2H_6O to different applied potentials (between 4 and -2 V), using a H_2/CO_2 ratio of 2, is displayed in Fig. 8. As can be observed in this figure, under these conditions the hydrogenation of CO_2 over the Cu electrocatalyst is significantly influenced by the applied potential. CO_2 conversion and selectivity to C_2H_6O exhibit a "volcano type" electrochemical behaviour, that is, they reach a maximum of 4.2 % and 87.1 %, respectively at a given potential of 0.5 V and 1 V, correspondingly.

As can be extracted from Fig. 8, formation of CH_3OH and C_2H_5OH is promoted at both highly positive and very negative potentials. Therefore, according to the previous findings, it seems to suggest that under this H_2/CO_2 ratio, at highly positive potentials, CH_3OH and C_2H_5OH formation takes place via hydrogenation of adsorbed CO resulting from hydrogen enhanced CO_2 dissociation (RWGS route), whereas, at very negative potentials, their formation occurs through the surface formate route [42, 65]. In both cases, selectivities to

methanol and ethanol exhibit also a “volcano type” electrochemical behaviour, i.e., they reach a maximum of 55.4 % and 19.7 % at 2.5 V and of 9 % and 7 % at -1.5 V (Θ_K=6.03, $PI_{kmethanol}$ = 5.5 and $PI_{Kethanol}$= 17). The variation of dimethyl ether selectivity vs. applied potential shows opposite tendency to that of methanol and ethanol selectivity, being a competition for the formation of the different hydrogenation products over the catalyst surface.

As can be obtained from Fig. 8, the optimum applied potential for CH_3OH and C_2H_5OH formation is about 2.5 V, which corresponds with an enhancement in its selectivity of up to 9 and 22 times, respectively, whereas a maximum improvement of 3.4 times in C_2H_6O selectivity is attained at 1 V (Θ_K=2.02 and $PI_{kdimethylether}$ = 2).

At positive potentials, CH_3OH selectivity is enhanced for a H_2/CO_2 of 2, probably because this value corresponds to the stoichiometric ratio required for CH_3OH formation via hydrogenation of CO resulting from hydrogen enhanced CO_2 dissociative adsorption. For the same reason, the formation of CH_2^* radical and derived species, such as ethanol, could be also improved under this H_2/CO_2 ratio.

As well, Fig. 9 depicts the steady state influence of applied potential variation (between 4 and -2 V) on CO_2 conversion and on the selectivity to CH_3OH, C_2H_5OH and C_2H_6O at a H_2/CO_2 ratio of 4.

As can be obtained from Fig. 9, under this H_2/CO_2 ratio, CO_2 conversion and selectivity to methanol, dimethyl ether and ethanol are enhanced on decreasing applied potential within the positive range. As indicated above, under application of high positive potentials, H_2 (electron donor) dissociative adsorption on Cu surface is favoured, being CO_2 (electron acceptor) adsorption the reaction limiting step. CO_2 dissociation is considered to be enhanced by the presence of adsorbed hydrogen. Hydrogenation of CO adsorbed species resulting from CO_2 dissociation leads to the formation to these oxygenated products. Decreasing catalyst potential results in the migration of potassium promoter species to the catalyst electrode favouring CO_2

(electron acceptor) adsorption on Cu surface, whereas H_2 dissociative adsorption is hindered. As a result, selectivity to CH_3OH, C_2H_5OH and C_2H_6O increases up to a maximum value of 8 %, 8,1 % and 70 % at about 1 V (Θ_K=2.02), 1.5 V (Θ_K=0.09) and 2 V, which corresponds with a maximum enhancement in its selectivity of up to 27, 4 and 1.7 times, respectively. In this case, selectivities to CH_3OH, C_2H_5OH and C_2H_6O showed similar trends against potential, because in spite of hydrogen dissociative adsorption is hindered on decreasing applied potentials, for H_2/CO_2 ratios of 4 (higher than the stoichiometric ratio) hydrogen coverage is always higher than that of species resulting from CO_2 dissociation [13] and thus CO adsorbed species can be gradually hydrogenated to the three species. Therefore, the competition between the different hydrogenation reactions is less pronounced.

However, the optimum potential for C_2H_6O formation is thought to be 1.5 V, which corresponds with a minimum in potassium coverage (of about 0.09) and with a maximum in current efficiency (around 7355.2) and promotion index (of about 36) for C_2H_6O formation, and given the simultaneous considerably high CO_2 conversion, which would result in high C_2H_6O yield.

A subsequent decrease in potential results in a decrease in selectivity to CH_3OH, C_2H_5OH and C_2H_6O, because the hydrogen evolution reaction is favoured, and the amount of hydrogen adsorbed on the surface is reduced and could limit CO_2 hydrogenation reactions. In addition, as more water is formed, the amount of surface CO generated by hydrogen enhanced CO_2 dissociation could decrease also trough the WGS reaction.

CO_2 conversion is relatively pronounced, up to about 25 % at 1 V (Θ_K= 2.02), but selectivities to CH_3OH and C_2H_5OH are rather low.

For better understanding of the influence of H_2/CO_2 ratio on catalyst performance and selectivity to the different target products, the potentiostatic variation of CO_2 conversion and selectivity to CH_3OH, C_2H_5OH and C_2H_6O is plotted for different H_2/CO_2 ratios in Figs. 10

(a) to (d), respectively. Results indicate that for applied potentials higher than 0.5 V, CO_2 conversion increases on increasing H_2/CO_2 ratio from 2 to 4, as a result of the increased hydrogen availability with respect to the stoichiometrically required for the synthesis of the different oxygenated products. Therefore, on increasing H_2/CO_2 ratio, the competition between the different hydrogenation reactions is less pronounced. On the one hand, for H_2/CO_2 ratios different from three, which matched with the theoretical stoichiometry in methanol synthesis by CO_2 hydrogenation, selectivity to methanol and ethanol decreased at negative potentials, whereas selectivity to dimethyl ether did at highly positive ones. This fact could be because the amount of surface hydrogen is in excess, for a H_2/CO_2 ratio of 4, and in defect, for a H_2/CO_2 ratio of 2, with respect to that required by stoichiometry for methanol synthesis via the formate route (at negative potentials) and for dimethyl ether synthesis through the RWGS pathway (at positive potentials), and, thus, the surface reactions could be restricted by the amount of CO_2 and H_2 adsorbed on the Cu surface, respectively [67].

On the other hand, for H_2/CO_2 ratios distinct from two, which is that required for stoichiometric synthesis of methanol from CO hydrogenation via the RWGS route, at highly positive potentials (above 1.5 V), selectivity to methanol was almost unaffected by H_2/CO_2 ratio [68] and ethanol selectivity decreased on decreasing H_2/CO_2 ratio [48], whereas selectivity to dimethyl ether decreased, at potentials below 1.5 V, on increasing H_2/CO_2 ratio.

For a H_2/CO_2 of two, selectivity to methanol (Fig. 10 b) [62] and ethanol (Fig. 10 c) showed a maximum and selectivity to dimethyl ether (Fig. 10 d) exhibited a minimum at 2.5 V.

Therefore selectivity to dimethyl ether follows an opposite trend vs. H_2/CO_2 ratio with respect to methanol and ethanol selectivity.

One of the main challenges for advancing CO_2 hydrogenation to fuels is increasing the energy efficiency of the process, i.e., decreasing the energy requirements for producing the products [4]. The trend is to maximize products yield with minimal energy input.

From the above commented results, it seems that the control of the yield of CH_3OH, C_2H_5OH and C_2H_6O can be carried out by modification of the applied potential, i.e., there is an optimum value of potential (or potassium surface coverage), at a given flow rate, temperature and H_2/CO_2 and ratio, which maximized CH_3OH, C_2H_5OH or C_2H_6O selectivity. Average values of potassium surface coverage, at steady state conditions, estimated for each applied potential are shown in Table 1. According to (3), only positive values of potassium coverage (negative values of current) has been included in Table 1, because negative values of potassium coverage (positive values of current) do not make sense unless represent the transfer of potassium ions from catalyst surface to the solid electrolyte.

The energy requirements for producing the different products can be evaluated from the values of current efficiency and energy cost calculated for each product formation (methanol, ethanol and dimethyl ether). The maximum values of current efficiency were obtained for 1.5 V (Θ_K of about 0.09) and resulted to be 87, 338 and 7355 for methanol, ethanol and dimethyl ether formation, respectively. Such a high current efficiency is a distinguishing feature of electrochemical promotion vs. electrocatalysis [6]. On the contrary, the corresponding minimum values of energy cost (kWh/Kg) associated with each product formation was 0.1, 0.03 and 0.0014, respectively. In most cases, the maximum in CH_3OH and C_2H_5OH selectivity coincides with a rather low CO_2 conversion value. On the contrary, as can be extracted from the obtained results, under some optimised conditions (mainly at 325 ºC, 522 l h^{-1}, 1.5 V and H_2/CO_2 ratios of 3 and 4), high values of C_2H_6O selectivity and CO_2 conversion can be obtained with a maximum in current efficiency and a minimum in energy cost and with low selectivities to the rest of the products (mainly CH_3OH and C_2H_5OH), which turn into higher

yield of finest dimethyl ether. The latter implies also lower cost associated with product purification. In addition, dimethyl ether is a liquid fuel susceptible of being directly used in diesel engines, therefore it may be considered as the best target product.

Practical application of CO_2 hydrogenation requires also the development of stable and durable systems under conditions representative of potential application, as well as their study under realistic conditions at an appropriate scale, which will be the subject of our forthcoming work. In fact, our future work will be focus on the study of the durability and stability of the system under selected operating conditions by monitoring of CO_2 conversion and selectivity to the different target products vs. time on stream and by correlation of these results with possible changes in catalytic behaviour and physicochemical properties of the catalyst as a result of the long term exposure to the testing gas, as a way also to identify and study any potential deactivation.

Although the aim of the work described in the present study was mainly to identify appropriate electrochemical catalyst systems and operating conditions for CO_2 hydrogenation to fuels, some information about system stability and durability can be extracted from the obtained results. No evidence signs of catalyst deactivation or corruption, apart from the slight sintering of Cu particles upon reduction and testing [36], could be found from XPS, XRD or SEM characterisation of the Cu film after testing. In addition, the resistance of both the Cu catalyst electrode and electrochemical cell remained the same after testing. Both facts seem to resemble certain stability of the system for moderate durations. Regarding the stability and durability of the system along surface cleaning/K surface doping cycles by varying potential, CO_2 conversion and selectivity to different target products obtained under unpromoted conditions (4 V) at the end and at the beginning of the cycles have been compared and the relative difference in CO_2 conversion and selectivities was mostly below about 6 %, which, could be ascribed to the experimental error in chromatographic analysis and not to

deactivation. In addition, the value of the current observed upon application of 4 V at the beginning and at the end of the cycles maintained in the same low value. Both facts seem to indicate also some durability of the system upon cleaning/doping cycles.

4. Conclusions

In this study, a Cu/K-βAl_2O_3/Au tubular electrochemical catalyst has been successfully prepared by electroless and characterised, both as prepared and after reduction and testing, by Scanning Electron Microscopy, X-Ray Photoelectron Spectroscopy and X-Ray Diffraction techniques.

The CO_2 hydrogenation over Cu in a potassium ion conducting membrane reactor can be electrochemically assisted under atmospheric pressure, at relatively low temperatures and high gas flow rates and under realistic postcombustion CO_2 capture exiting gas compositions. Selectivity to the different target fuels can be modulated by modifying applied potential under given operating conditions.

The hydrogenation of CO_2 over the Cu catalyst leads mainly to the formation of methanol, dimethyl ether and ethanol, but CO, CH_4, C_2+C_3 hydrocarbons, formic acid and acetic acid were also detected to be formed.

Selectivities to CH_3OH, C_2H_5OH and C_2H_6O were electrochemically enhanced up to a maximum of 34, 22 and 3.4 times, respectively.

A temperature value of 325 ºC was selected to be the optimum for the electrochemically assisted CO_2 hydrogenation process.

Increasing gas flow rate, for a given H_2/CO_2 ratio of 3 and at 325 ºC, resulted in an increase in CO_2 conversion and dimethyl ether selectivity and in a decrease in both ethanol selectivity and the maximum of methanol selectivity, which shifts to more negative potentials. The

increase in gas flow rate was found also to favour dimethyl ether synthesis reaction at the expense of methanol and ethanol formation.

Results obtained at different H_2/CO_2 ratios, at 522 l h^{-1} and 325 ºC, showed that the maximum in CO_2 conversion increases with H_2/CO_2 ratio, whereas the maximum in selectivity to the different oxygenates is obtained for a H_2/CO_2 ratio of 2, being 55.4 %, 19.7 % and 87.1 % for CH_3OH, C_2H_5OH and C_2H_6O, respectively. Selectivity to dimethyl ether follows an opposite trend vs. H_2/CO_2 ratio with respect to methanol and ethanol ones.

Therefore, this study addresses some scale-up aspects, such as operation at high flow rates and atmospheric pressure, under realistic gas compositions and using catalyst-electrode configurations easily adaptable to the existing catalytic devices (conventional flow reactors), based on a cheap, widespread and non-precious Cu catalyst, and prepared by commercial ready procedures, which may have an impact on the potential practical application of the process for CO_2 recycling, contributing not only to controlling the global "Green-house Effect", but also to the availability of fuel sources for the future.

Acknowledgements

The authors acknowledge support from Ministerio de Ciencia e Innovación of Spain (Project ENE2010-15569). Pedro J. Martinez is grateful to Ministerio de Ciencia e Innovación of Spain for the research grant BES-2011-046902.

References

[1] G.A. Olah, A. Goeppert, G.K.S. Prakash, J. Org. Chem. 74 (2009) 487–498.

[2] F. Ocampo, B. Louis, A. Kiennemann, A. C. Roger, Mater. Sci. Eng. 19 (2011) 1–11.

[3] S.K. Hoekman, A. Broch, C. Robbins, R. Purcell, Int. J. Greenhouse Gas Control 4 (2010) 44–50.

[4] D.T. Whipple, P.J. Kenis, J. Phys. Chem. Lett. (2010) 3451–3458.

[5] N.A.M. Zabidi, M.Z. Ramli, F.K. Chong, Journal of Chemistry and Chemical Engineering, 3 (2009) 1-6.

[6] C.G. Vayenas, S. Bebelis, C. Pliangos, S. Brosda, D. Tsiplakides, Electrochemical Activation of Catalysis: Promotion, Electrochemical Promotion and Metal-Support Interactions, Kluwer Academic/Plenum Publishers, New York, 2001.

[7] G. Karagiannakis, S. Zisekas, M. Stoukides, Solid State Ionics 162–163 (2003) 313–318.

[8] E.I. Papaioannou, S. Souentie, A. Hammad, C.G. Vayenas, Catal. Today 146 (2009) 336–344.

[9] G. Pekridis, K. Kalimeri, N. Kaklidis, E. Vakouftsi, E.F. Iliopoulou, C. Athanasiou, G.E. Marnellos, Catal. Today 127 (2007) 337–346.

[10] E. Ruiz, D. Cillero, P.J. Martínez, A. Morales, G. San Vicente, G. de Diego, J.M. Sánchez, Catal. Today 210 (2012) 55–66.

[11] S. Bebelis , H. Karisali, C.G.Vayenas, Solid State Ionic 179 (2008) 1391–1395.

[12] S. Bebelis, H. Karasali, C.G. Vayenas, J. Appl. Electrochem. 38 (2008) 1127–1133.

[13] D. Theleritis, S. Souentie, A. Siokou, A. Katsaounis, C.G. Vayenas, ACS Catal. 2 (2012) 770–780.

[14] D. Theleritis, M. Makri, S. Souentie, A. Caravaca, A. Katsaounis, C.G. Vayenas, ChemElectroChem (2014) (published online), doi: 10.1002/celc.201300185.

[15] V. Jiménez, C. Jiménez-Borja, P. Sánchez, A. Romero, E.I. Papaioannou, D. Theleritis, S. Souentie, S. Brosda, J.L. Valverde, Appl. Catal., B 107 (2011) 210–220.

[16] D. Tsiplakides, S. Balomenou, Chem. Ind. Chem. Eng. Q. 14 (2008) 97–105.

[17] D. Tsiplakides, S. Balomenou, Catal. Today 146 (2009) 312–318.

[18] A. Anastasijevic, Catal. Today 146 (2009) 308–311.

[19] S. Hadenfeldt, C. Benndorf, A. Stricker, M. Töwe, Surf. Sci. 352-354 (1996) 295–299.

[20] H.J. Freund, M.W. Roberts, Surf. Sci. Rep. 25 (1996) 225–273.

[21] J. Onsgaard, L. Thomsen, S.V. Hoffmann, P.J. Godowski, Vacuum 81 (2006) 25–31.

[22] J. Onsgaard, S.V. Hoffmann, P. Moller, P.J. Godowski, J.B. Wagner, G. Paolucci, A. Baraldi, G. Comelli, A. Groso, ChemPhysChem 4 (2003) 466–473.

[23] J. Onsgaard, P.J. Godowski, J. Nerlov, S.V. Hoffmann, Surf. Sci. 398 (1998) 318–331.

[24] J.R. Davis, ASM Specialty Handbook: Copper and Copper alloys, ASM International, Ohio, 2001.

[25] F. Inoue, T. H. Philipsen, A. Radisic, S. Armini, Y. Civale, P. Leunissen, M. Kondo, E. Webb, S. Shingubara, Electrochim. Acta 100 (2013) 203–211.

[26] S. Komatsu, M. Tanaka, A. Okumura, A. Kungi, Electrochim. Acta 40 (1995) 745–753.

[27] M.T. Schaal, A.Y. Metcalf, J.H. Montoya, J.P. Wilkinson, C.C. Stork, C.T. Willians, J.R. Monnier, Catal. Today 123 (2007) 142–150.

[28] J.M. Cordoba, M. Oden, Surf. Coat. Technol. 203 (2009) 3459–3464.

[29] Z.Y. Wen, Z.X. Lin, K.G. Chen, Solid State Ionics 95 (1997) 295–300.

[30] C.K. Kuo, N.D. Patel, A. Tan, P. Sarkar, P.S. Nicholson, Solid State Ionics 53–56 (1992) 564–570.

[31] P. Vernoux, F. Gaillard, C. Lopez, E. Siebert, Solid State Ionics 175 (2004) 609.

[32] C.S. Chen, J.H. You, J.H. Lin, Y.Y. Chen, Catal. Commun. 9 (2008) 2381–2385.

[33] X. Yao, Q. Yu, Z. Ji, Y. Lv, Y. Cao, C. Tang, F. Gao, L. Dong, Y. Chen, Appl. Catal. B

[34] A. de Lucas Consuegra, A. Caravaca, J. Gonzalez-Cobos, J. L. Valverde, F. Dorado, Catal. Commun. 15 (2011) 6–9.

[35] C. Guizard, A. Princivalle, Catal. Today 146 (2009) 367–377.

[36] A. Basonde, B. Tidona, P.R. von Rohr, A. Urakawa, Catal. Sci. Technol. 3 (2013) 767–778.

[37] A. Dankdekar, M.A. Vannice, J. Catal. 178 (1998) 621–639.

[38] V.K. Kaushik, C. Sivaraj, P.K. Rao, Appl. Surf. Sci. 51 (1991) 27–33.

[39] A. Karelovic, A. Bargibant, C. Fernandez, P. Ruiz, Catal. Today 197 (2012) 109–118.

[40] C.S. Chen, W.H. Cheng, S.S. Lin, Catal. Letters 68 (2000) 45–48.

[41] C.S. Chen, W.H. Cheng, Catal. Letters 80 (2002) 121–126.

[42] C.S. Chen, W.H. Cheng, S.S. Lin, Appl. Catal. A 238 (2003) 55–67.

[43] M. Le, M. Ren, Z. Zhang, P.T. Sprunger, R.L. Kurtz, J.C. Flake, J. Electrochem. Soc. 158 (2011) E45–E49.

[44] I.A. Fisher, A.T. Bell, J. Catal. 172 (1997) 222–237.

[45] K.D. Jung, A.T. Bell, J. Catal. 193 (2000) 207–223.

[46] Y. Souma, H. Ando, M. Fujiwara, R. Kieffer, Energy Convers. Manage. 36 (1995) 593–596.

[47] R. Sahki, O. Benlounes, O. Chérifi, R. Thouvenot, M.M. Bettahar, S. Hocine, React. Kinet. Mech. Catal. 103 (2011) 391–403.

[48] W. Hua, W. Li, S. Xuelian, Coal Chem. Ind. 33 (2005) 30–35.

[49] M. Kasaie, M. Sohrabi, J. Mex. Chem. Soc. 53 (2009) 233–238.

[50] S. Brosda, C.G. Vayenas, J. Wei, Appl. Catal. B 68 (2006) 109–124.

[51] S. Yin, Q. Ge, Catal. Today 194 (2012) 30–37.

[52] Q.J. Hong, Z.P. Liu, Surf. Sci. 604 (2010) 1869–1876.

[53] D.B. Clarke, A.T. Bell. J. Catal. 154 (1995) 314–328.

[54] H. Arakawa, J.L. Dubois, K. Sayama, Energy Convers. Manage. 33 (1992) 521–528.

[55] H. Kusama, K. Okabe, K. Sayama, H. Arakawa , Catal. Today 28 (1996) 261–266.

[56] P. Dube, G.M. Brisard, J. Electroanal. Chem. 582 (2005) 230–240.

[57] G.M. Brisard, A.P.M. Camargo, F.C. Nart, T. Iwasita, Electrochem. Commun. 3 (2001) 603–607.

[58] R.A. Hadden, H.D. Vanderell, K.C. Waugh, G. Webb, Catal. Letters 1 (1988) 27–34.

[59] J. Nakamura, J.A. Rodriguez, C.T. Campbell, J. Phys. Condens. Matter 1 (1989) SB149–SB160.

[60] M. Maack, H. Friis-Jensen, S. Sckerl, J.H. Larsen, I. Chorkendorff, Topic Catal. 22 (2003) 151–160.

[61] S. Li, A. Li, S. Krishnamoorthy, E. Iglesia, Catal. Letters 77 (2001) 197–205.

[62] P.B. Rasmussen, M. Kazuta, I. Chorkendorff, Surf. Sci. 318 (1994) 267–280.

[63] P. Gao, F. Li, F. Xiao, N. Zhao, W. Wei, L. Zhong, Y. Sun, Catal. Today 194 (2012) 9–15.

[64] W. Wang, J. Gong, Front. Chem. Sci. Eng. 5 (2011) 2–10.

[65] K.C. Waugh, Solid State Ionics 168 (2004) 327–342.

[66] Z. Huo, M. Hu, X. Zeng, J. Yun, F. Jin, Catal. Today 194 (2012) 25–29.

[67] M. Xu, M.J.L. Gines, A.M. Hilmen, B.L. Stephens, E. Iglesia, J. Catal. 171 (1997) 130–147.

[68] J. Wu, M. Saito, M. Takeuchi, T. Watanabe, Appl. Catal. A 218 (2001) 235–240.

(a) (b)

Fig. 1. SEM micrographs of the Cu catalyst-working electrode film: (a) as prepared, (b) after reduction and testing.

Fig. 2. XRD analysis of the Cu catalyst-working electrode film: (a) as prepared, (b) after reduction and testing.

Fig. 3. Influence of temperature on (■) CO_2 conversion and on selectivity to (●) CH_3OH, (▲) C_2H_5OH and (▼) C_2H_6O. (a) over a clean Cu surface (4V), (b) under anodic polarization (2V), (c) without polarization (0V) and (d) under cathodic polarization (-2V). (90 l h^{-1}, $H_2/CO_2 = 3$).

Fig. 4. Influence of temperature on (a) CO_2 conversion and on selectivity to (b) CH_3OH, (c) C_2H_5OH and (d) C_2H_6O. (■) over a clean Cu surface (4V), (●) under anodic polarization (2V), (▲) without polarization (0V) and (▼) under cathodic polarization (-2V). (90 l h^{-1}, H_2/CO_2 = 3).

Fig. 5. Influence of the applied potential on (■) CO_2 conversion and on selectivity to (●) CH_3OH, (▲) C_2H_5OH and (▼) C_2H_6O (90 l h^{-1}, $H_2/CO_2 = 3$, 325 ºC).

Fig. 6. Influence of the applied potential on (■) CO_2 conversion, on selectivity to (●) CH_3OH, (▲) C_2H_5OH, (▼) C_2H_6O and (◆) CO and on carbon balance (★). (522 l h^{-1}, $H_2/CO_2 = 3$, 325 ºC)

Fig. 7. Effect of gas flow rate on the potentiostatic variation of (a) CO_2 conversion and selectivity to (b) CH_3OH, (c) C_2H_5OH and (d) C_2H_6O. (■) 522 l h^{-1} and (●) 90 l h^{-1}. (H_2/CO_2 = 3, 325 ºC).

Fig. 8. Influence of the applied potential on (■) CO_2 conversion and on selectivity to (●) CH_3OH, (▲) C_2H_5OH and (▼) C_2H_6O. (522 l h^{-1}, H_2/CO_2 = 2, 325 ºC).

Fig. 9. Influence of the applied potential on (■) CO_2 conversion and on selectivity to (●) CH_3OH, (▲) C_2H_5OH and (▼) C_2H_6O. (522 l h^{-1}, H_2/CO_2 = 4, 325 ºC).

Fig. 10. Effect of H_2/CO_2 ratio on the potentiostatic variation of (a) CO_2 conversion and selectivity to (b) CH_3OH, (c) C_2H_5OH and (d) C_2H_6O. (■) H_2/CO_2 = 4, (●) H_2/CO_2 = 3 and (▲) H_2/CO_2 = 2. (522 l h^{-1}, 325 ºC).

Table 1

Applied potential, observed current and potassium coverage at steady state conditions

Potential (V)	Current (A)	Θ_K
4	0.039	N/A
3.5	0.042	N/A
3	0.027	N/A
2.5	0.016	N/A
2	0.0072	N/A
1.5	-0.00058	0.09
1	-0.013	2.02
0.5	-0.015	2.32
-0.5	-0.055	8.56
-1	-0.057	8.94
-1.5	-0.039	6.03
-2	-0.034	5.23

Fig.1(a).tif
Click here to download high resolution image

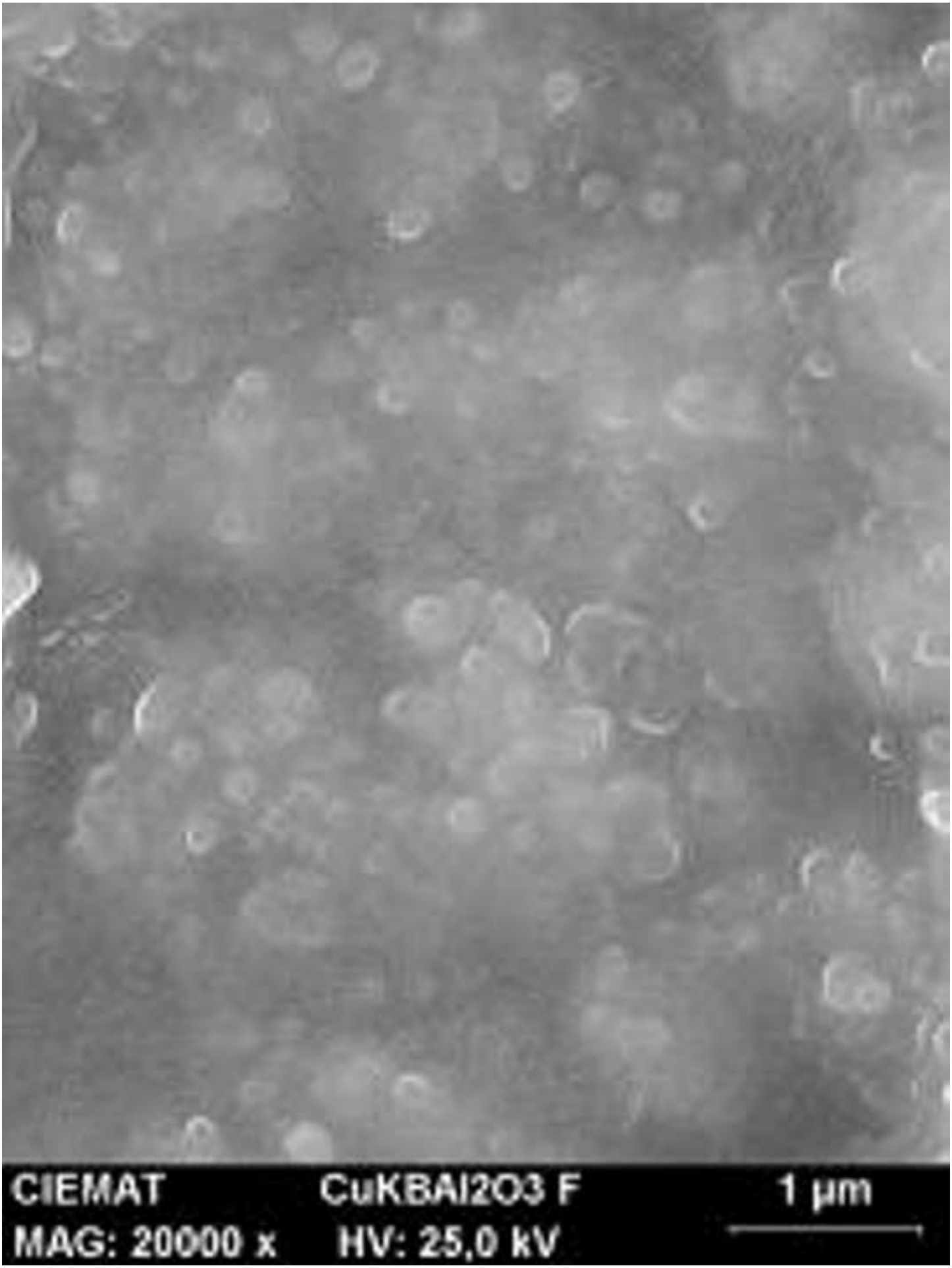

Fig.1(b).tif
Click here to download high resolution image

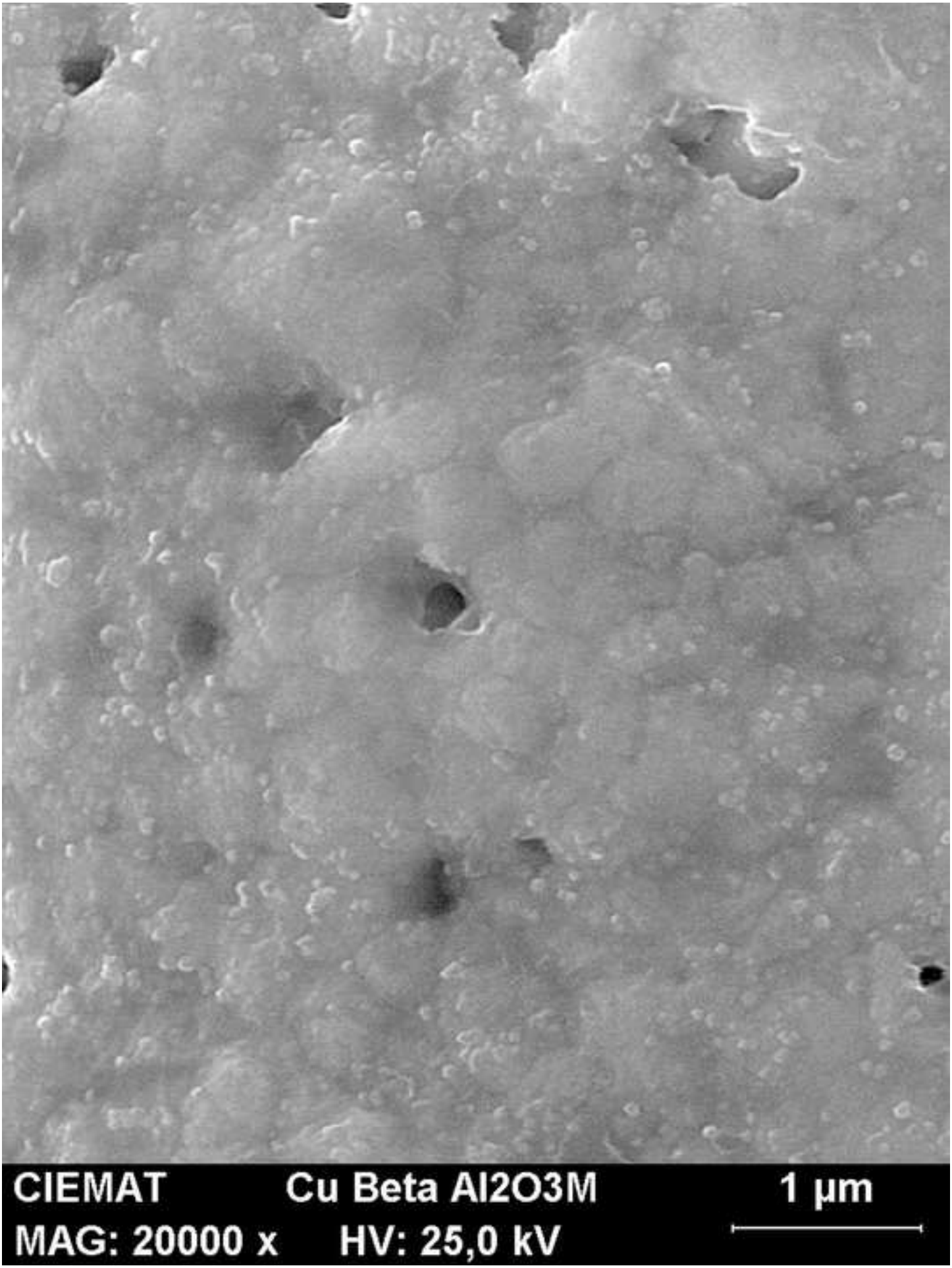

Fig.2(a).TIF
Click here to download high resolution image

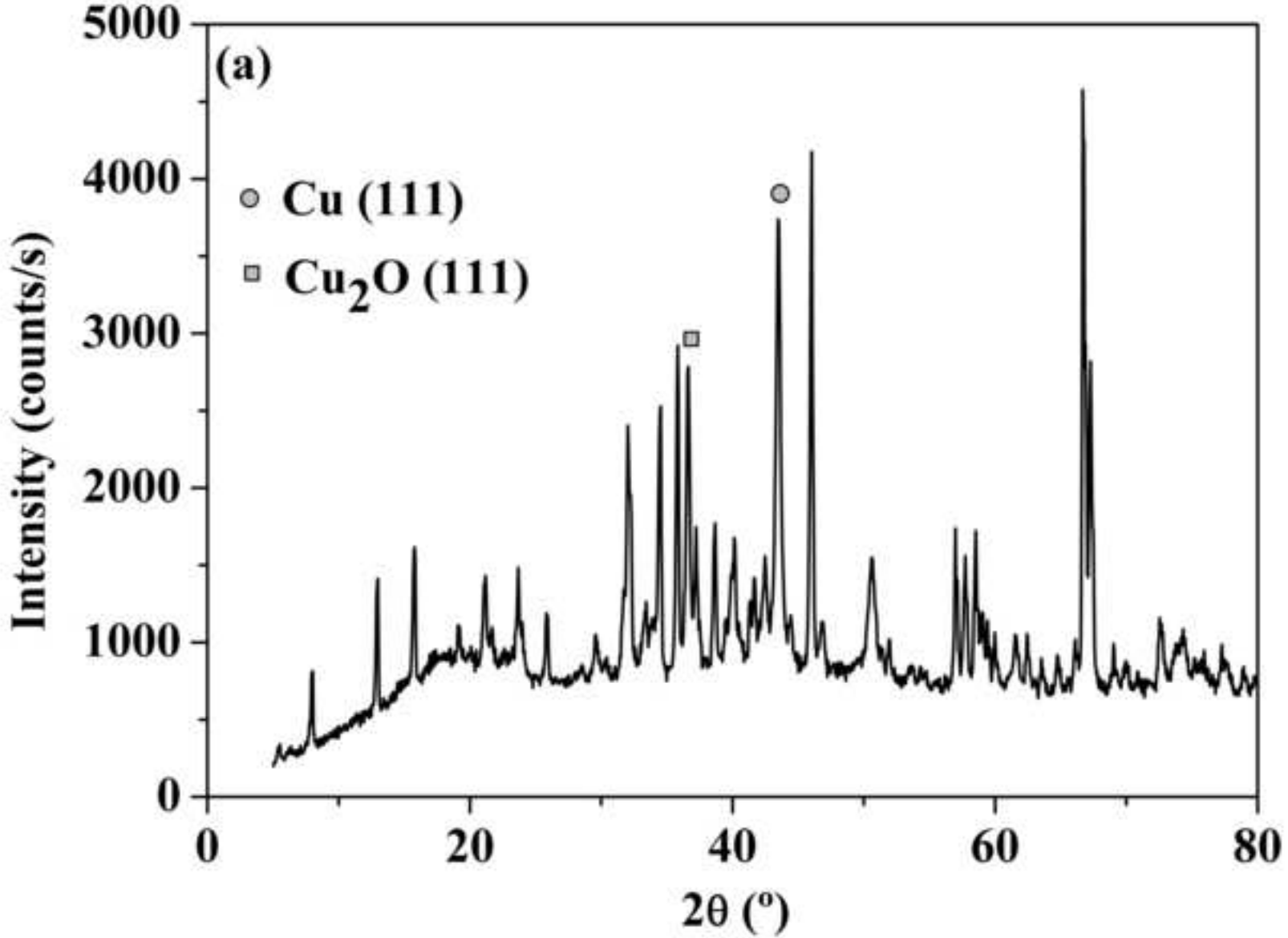

Fig.2(b).TIF
Click here to download high resolution image

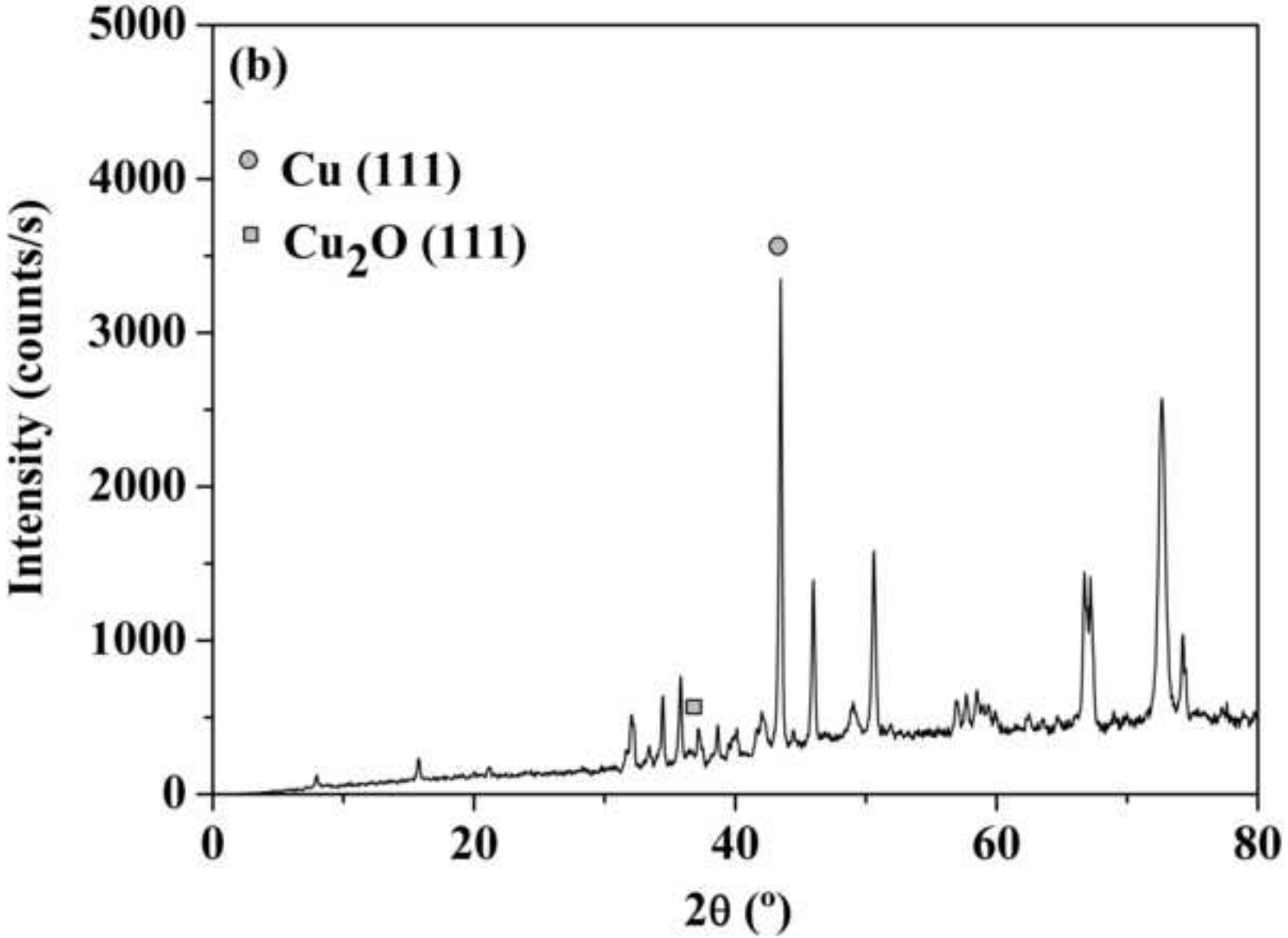

Fig.3(a).TIF
Click here to download high resolution image

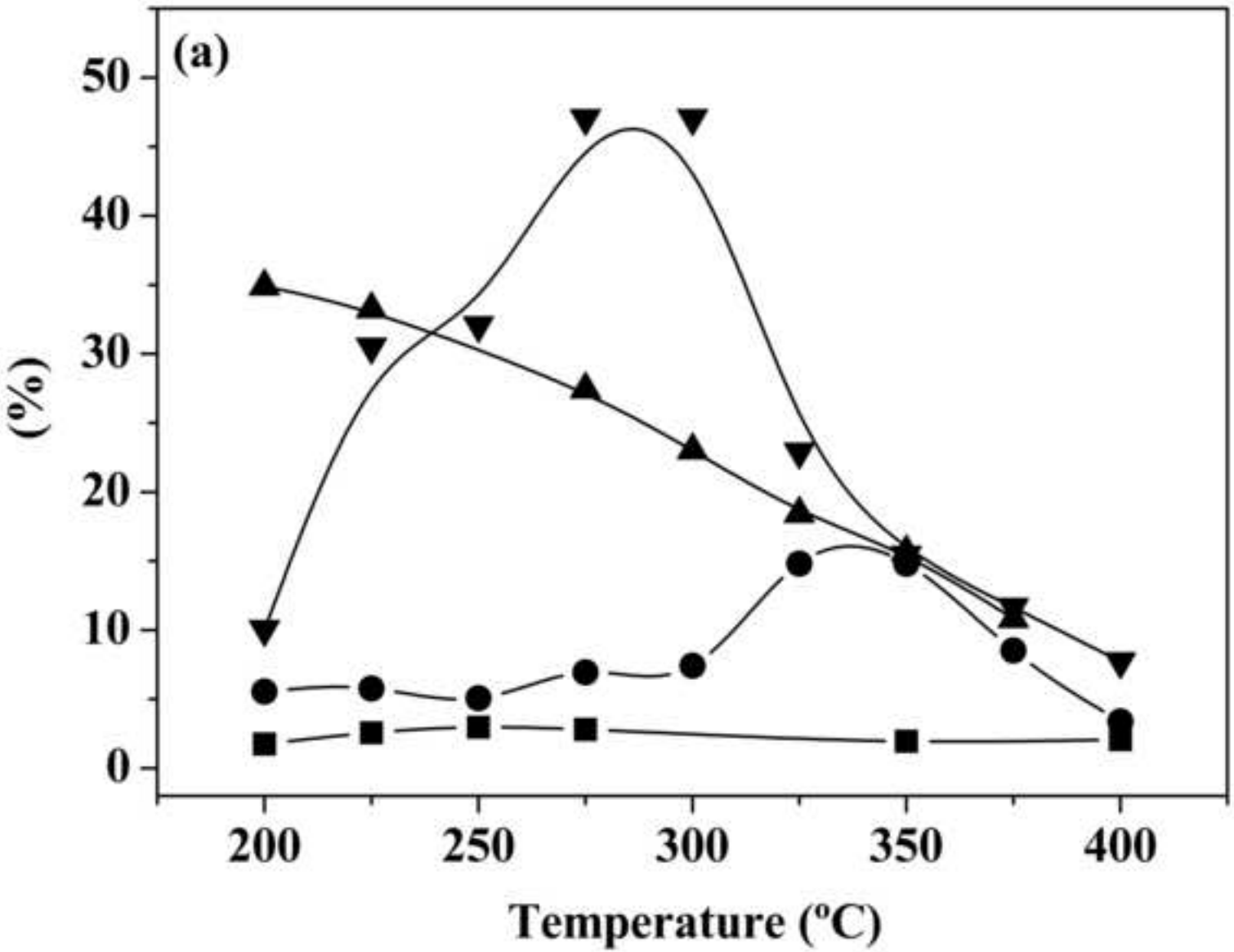

Fig.3(b).TIF
Click here to download high resolution image

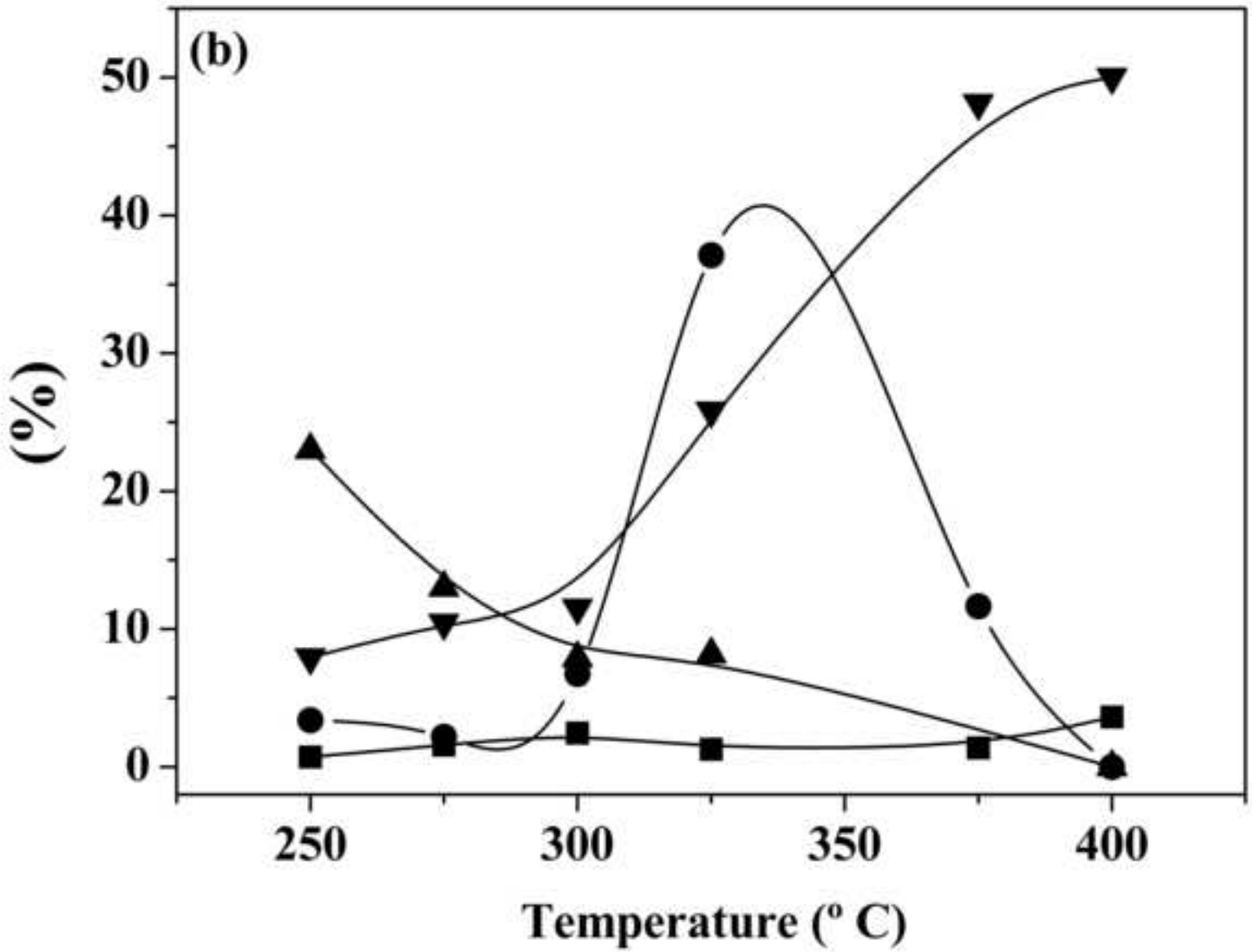

Fig.3(c).TIF
Click here to download high resolution image

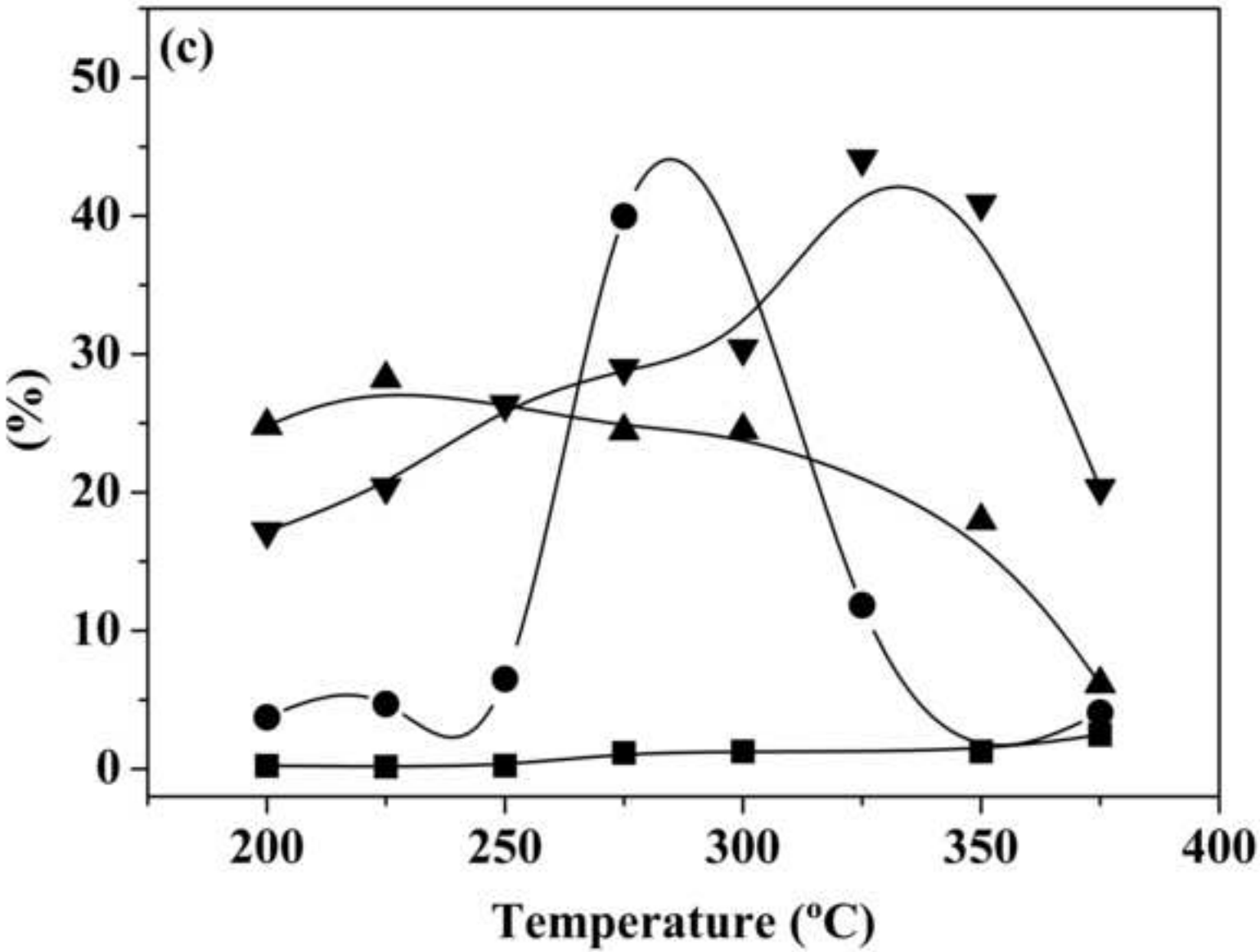

Fig.3(d).TIF
Click here to download high resolution image

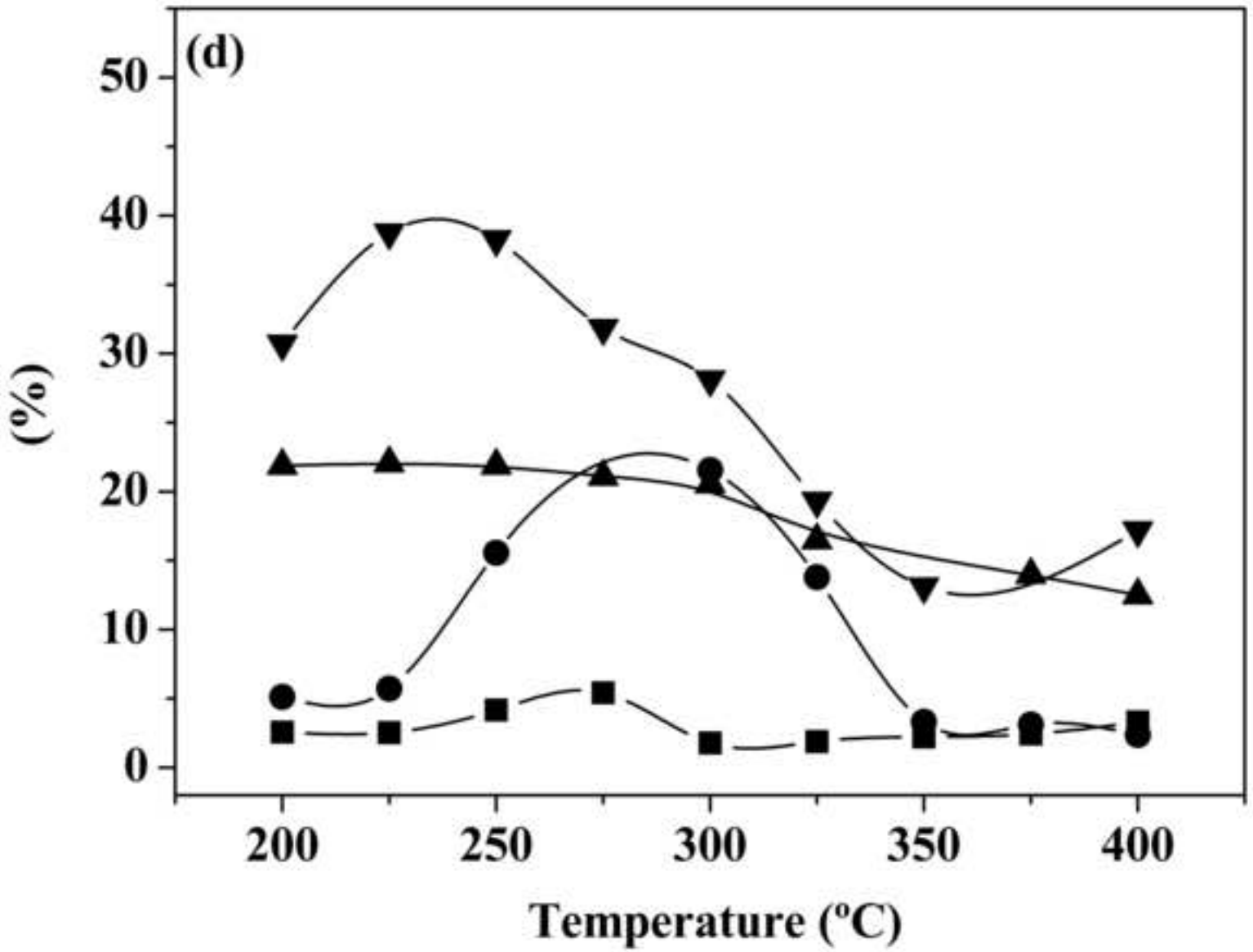

Fig.4(a).TIF
Click here to download high resolution image

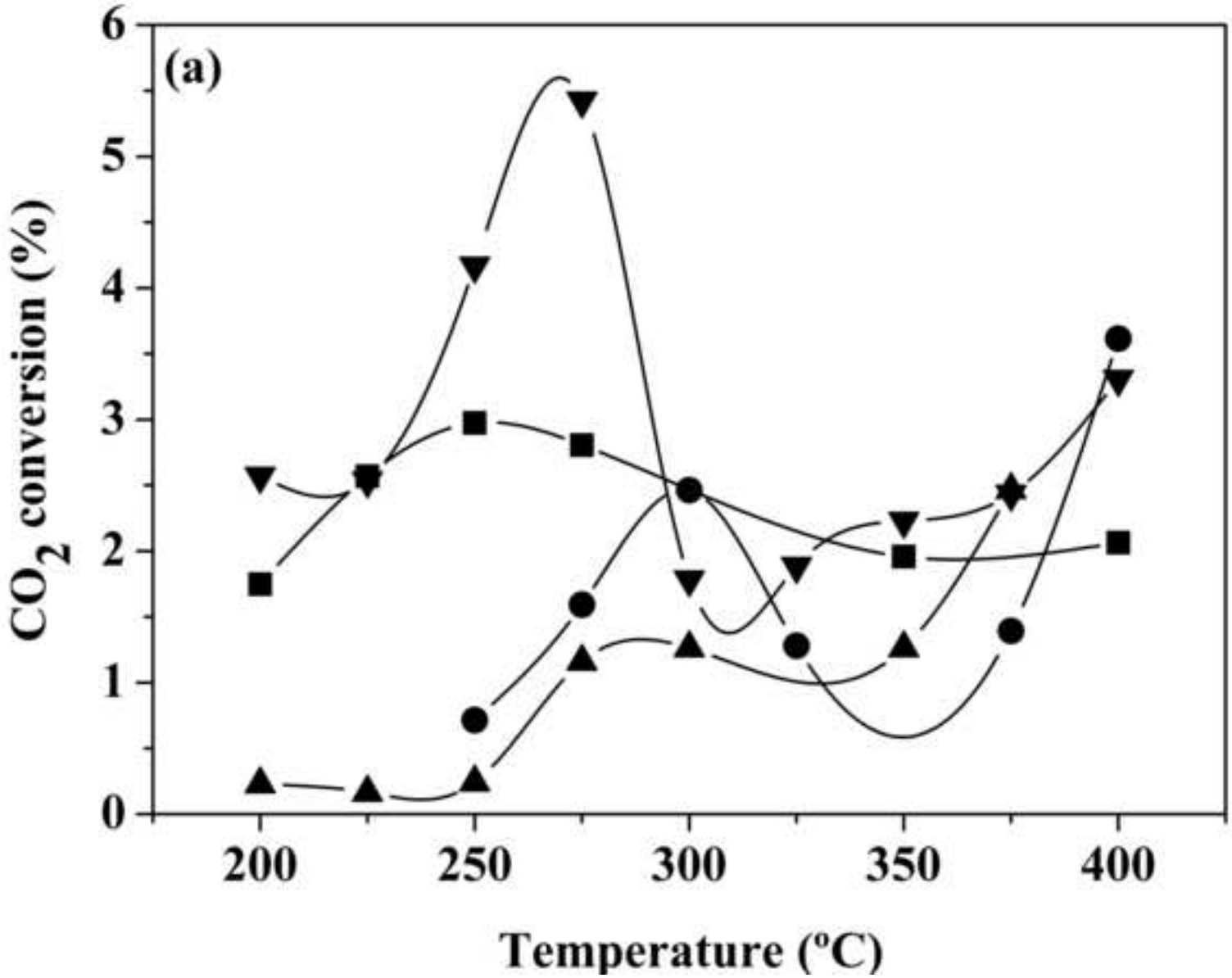

Fig.4(b).TIF
Click here to download high resolution image

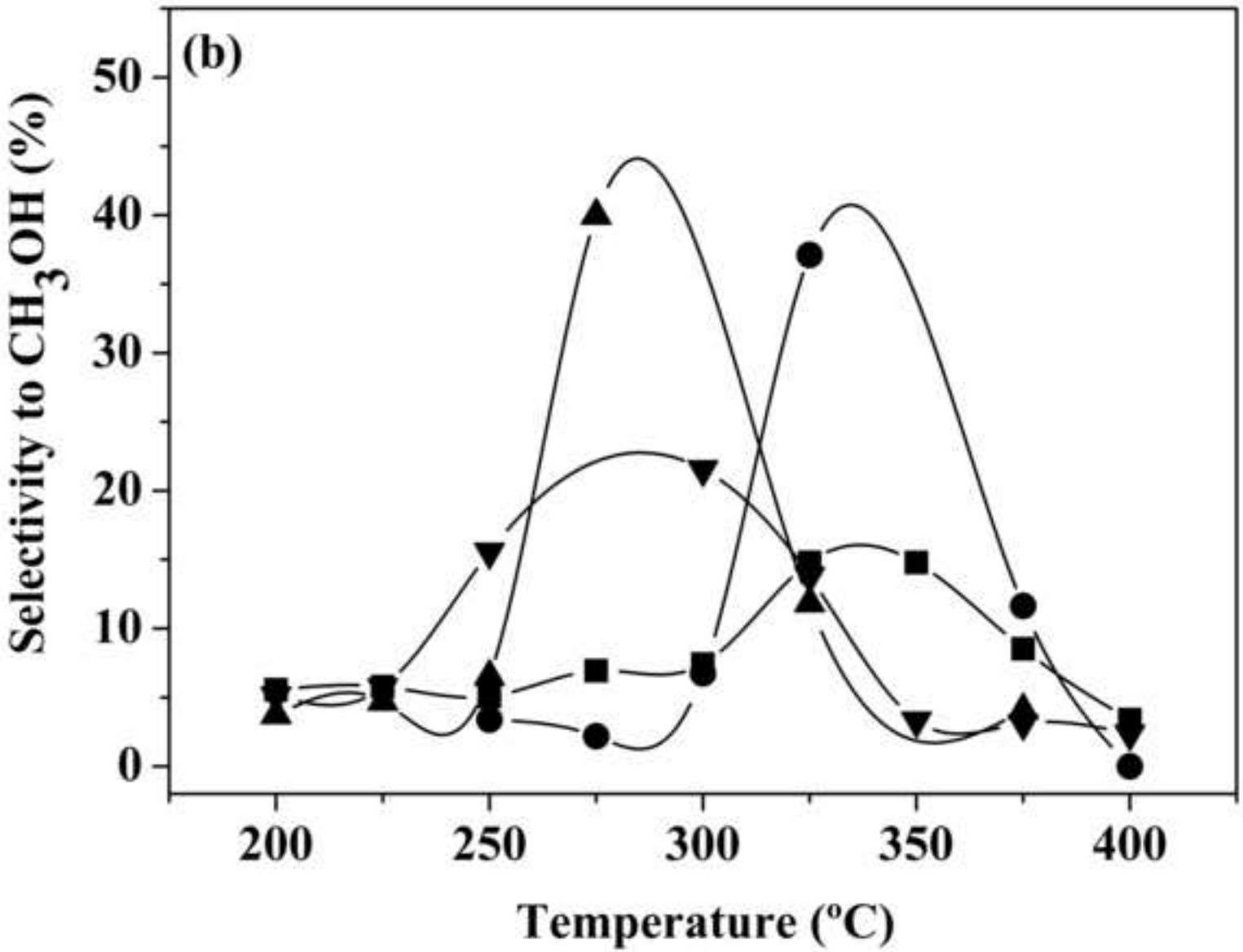

Fig.4(c).TIF
Click here to download high resolution image

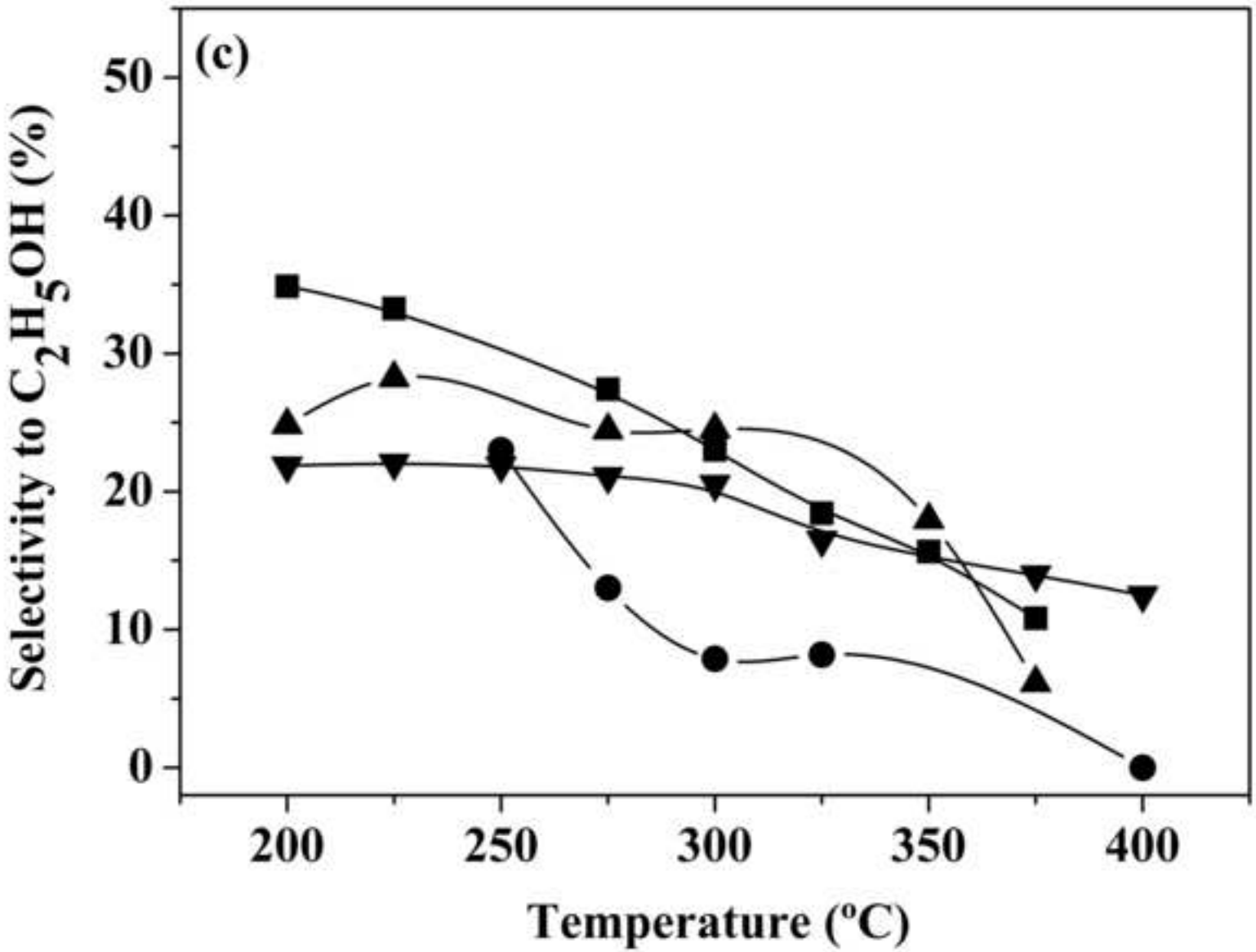

Fig.4(d).TIF
Click here to download high resolution image

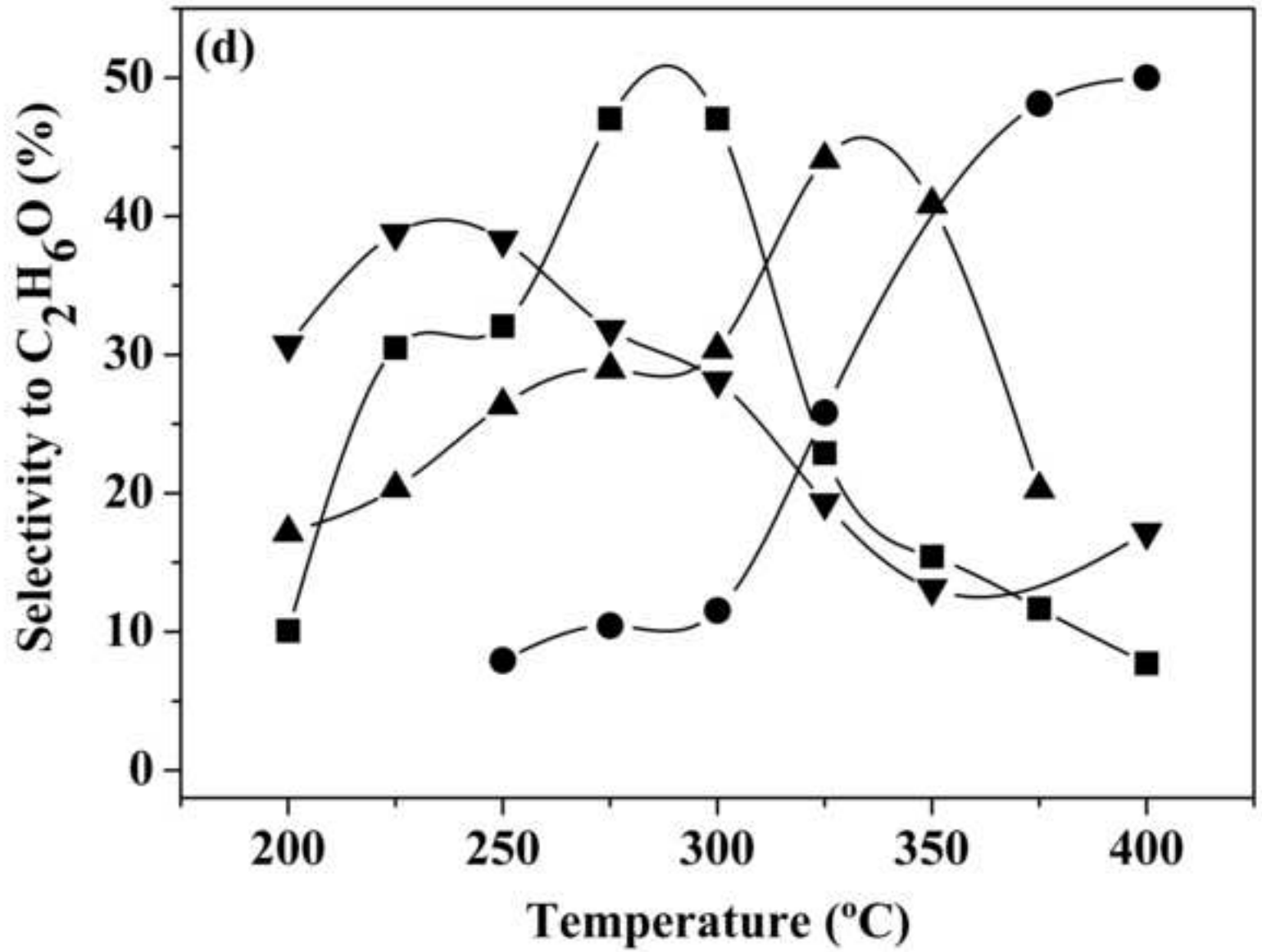

Fig.5.TIF

Click here to download high resolution image

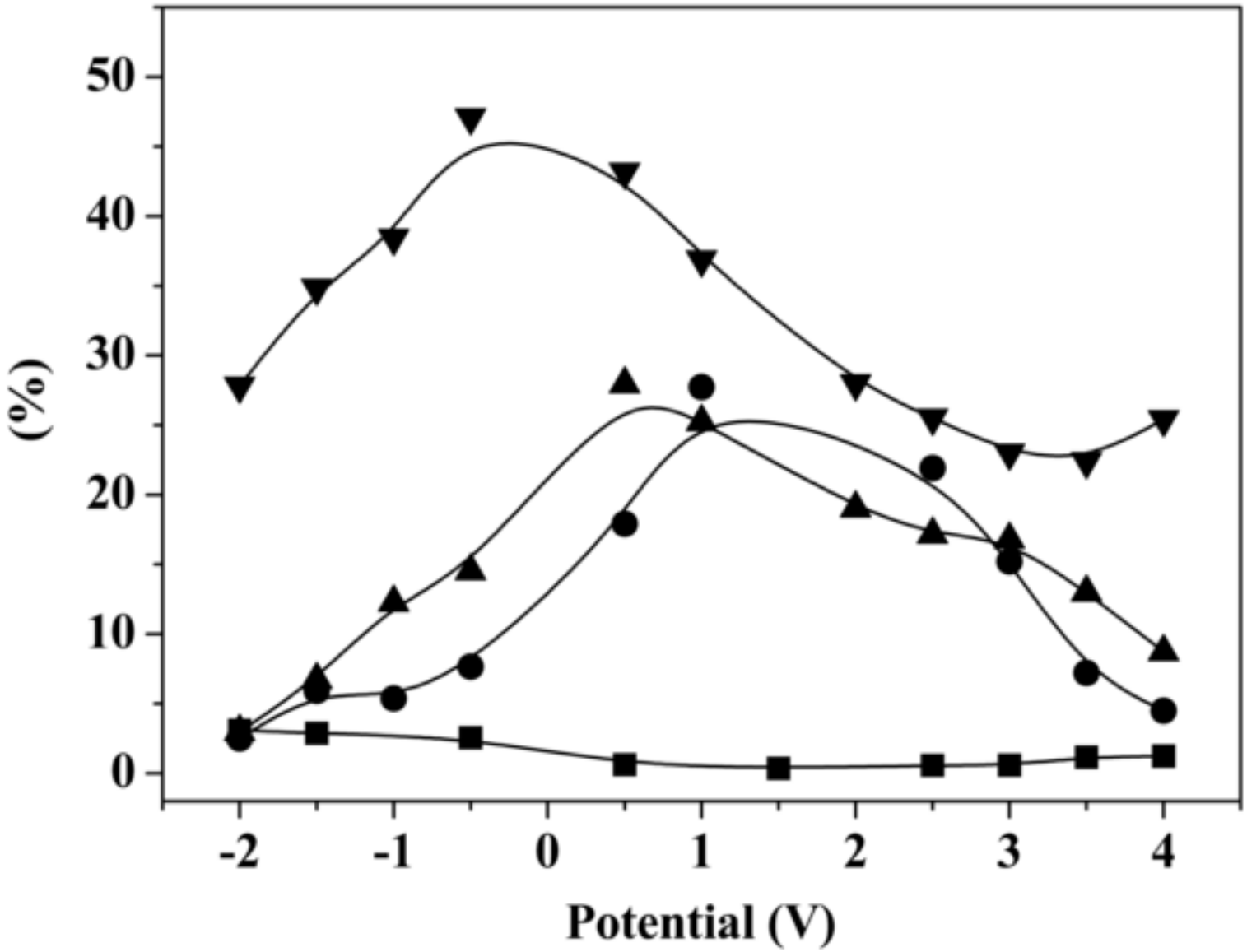

Figure
Click here to download high resolution image

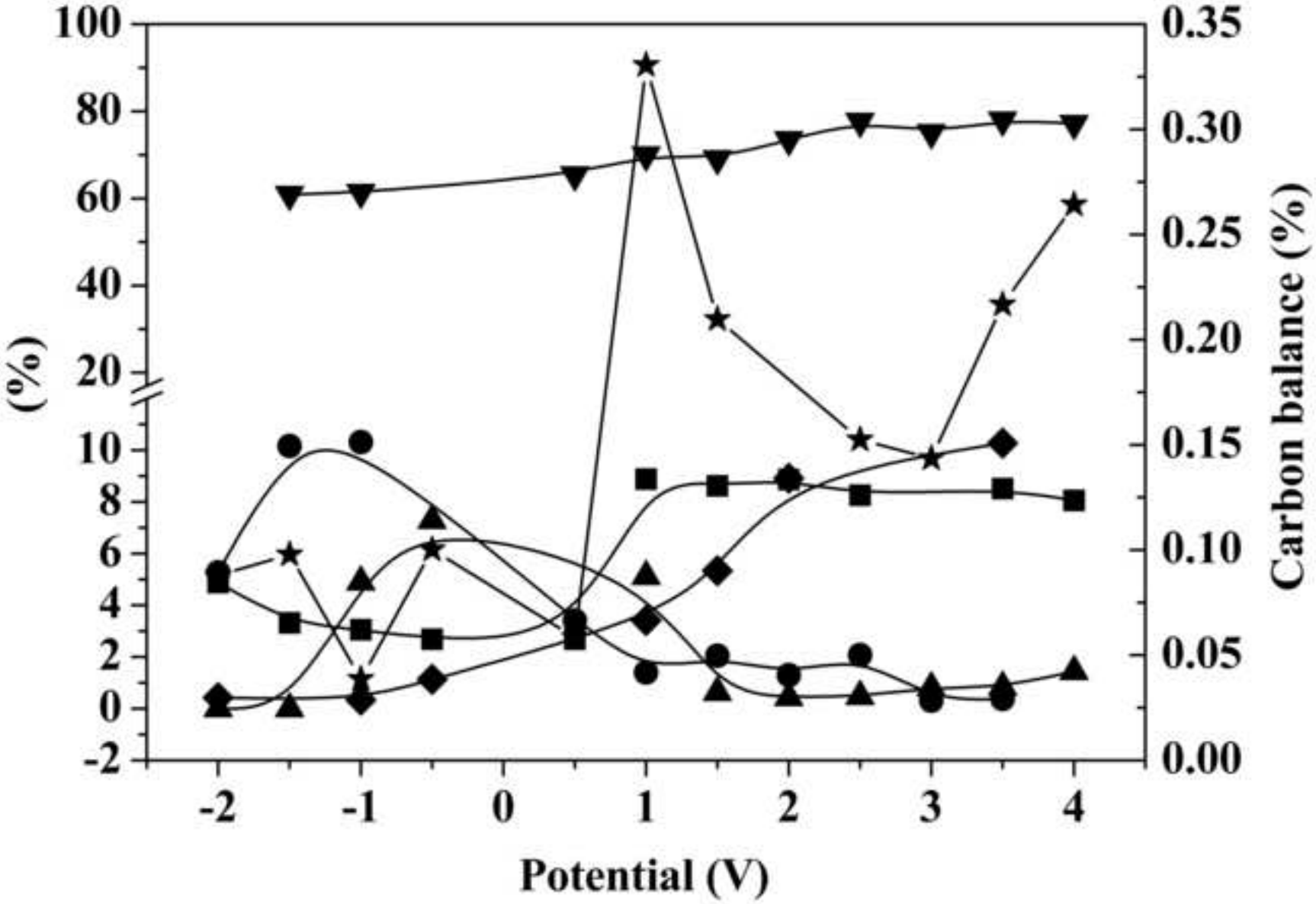

Fig.7(a).TIF
Click here to download high resolution image

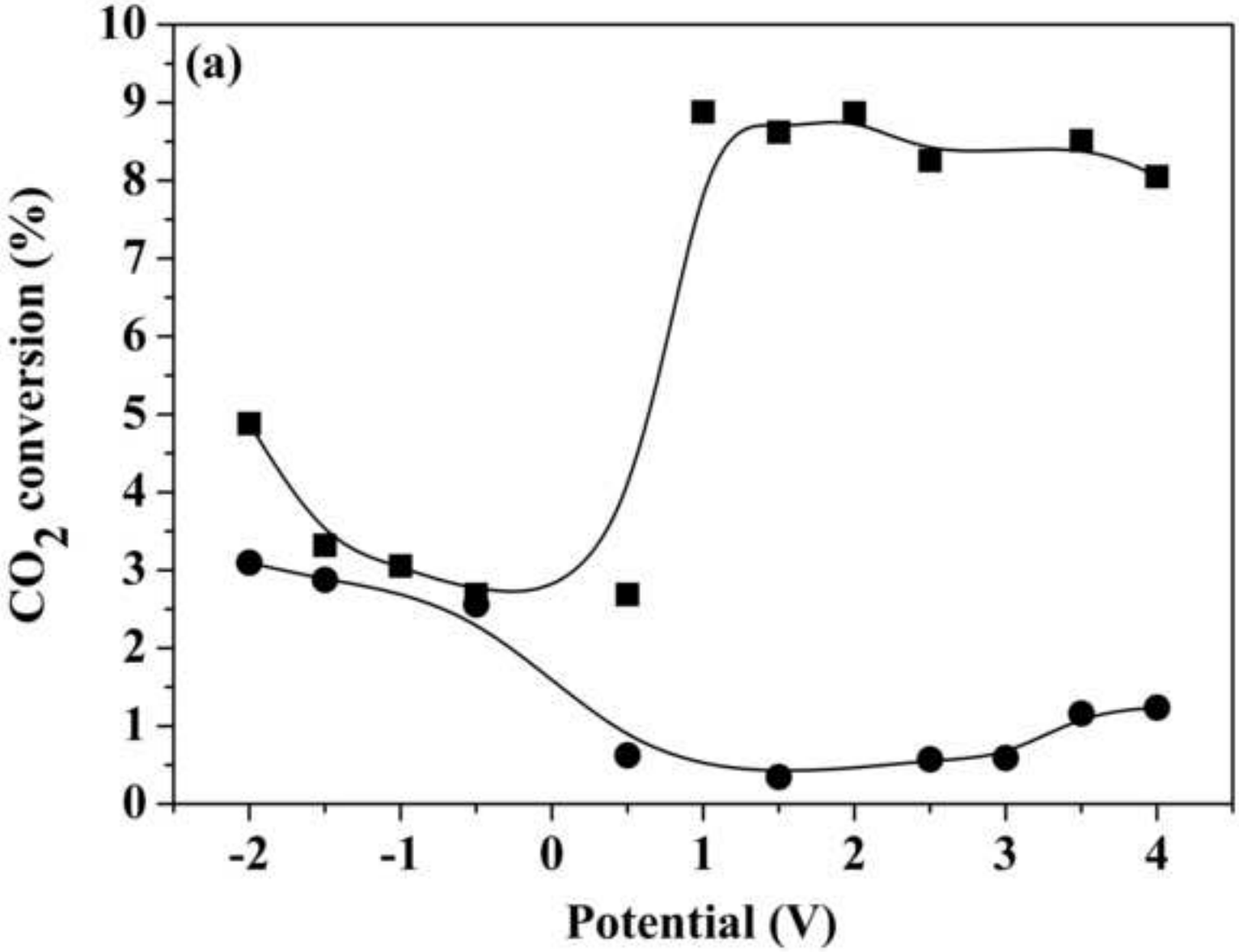

Fig.7(b).TIF
Click here to download high resolution image

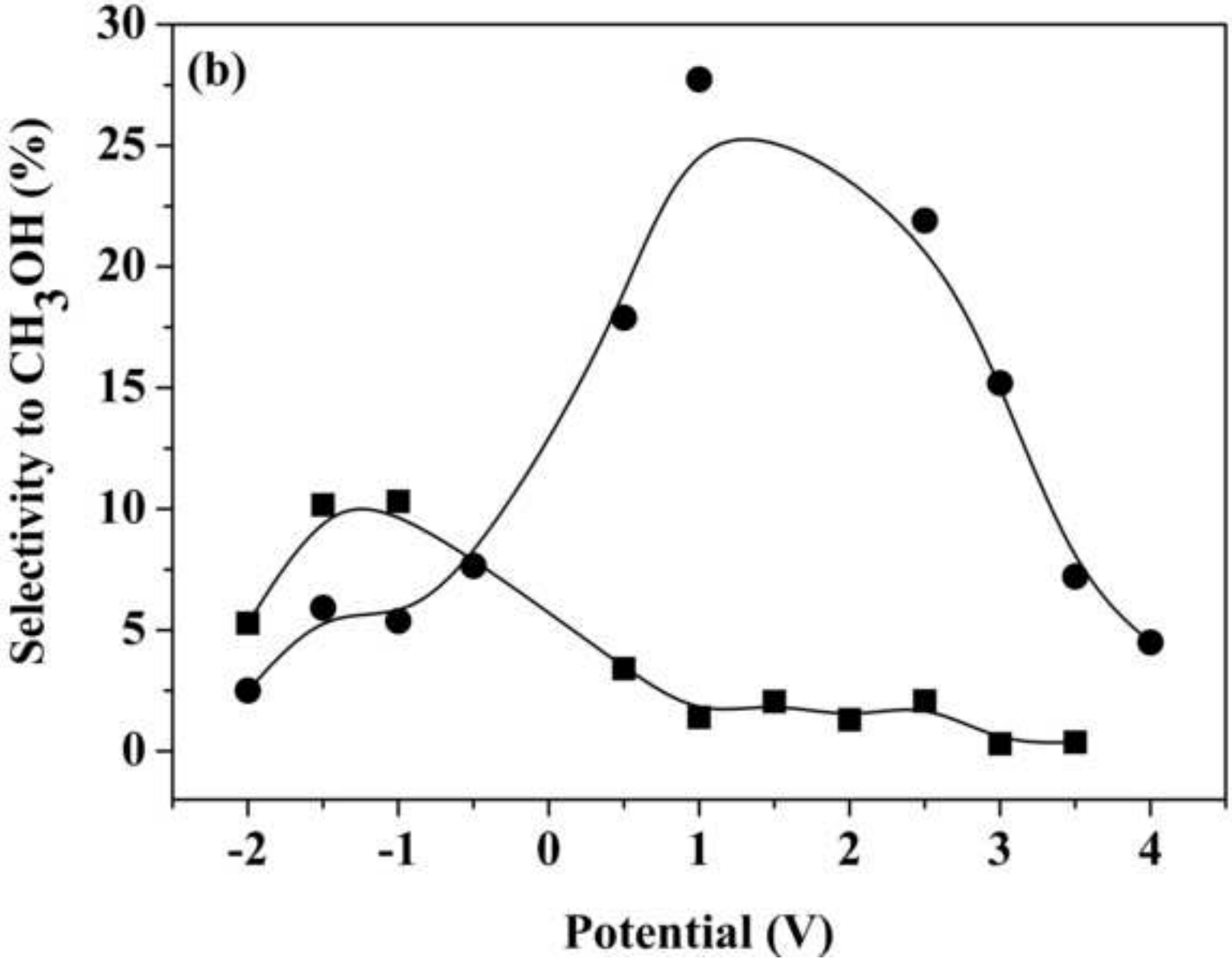

Fig.7(c).TIF
Click here to download high resolution image

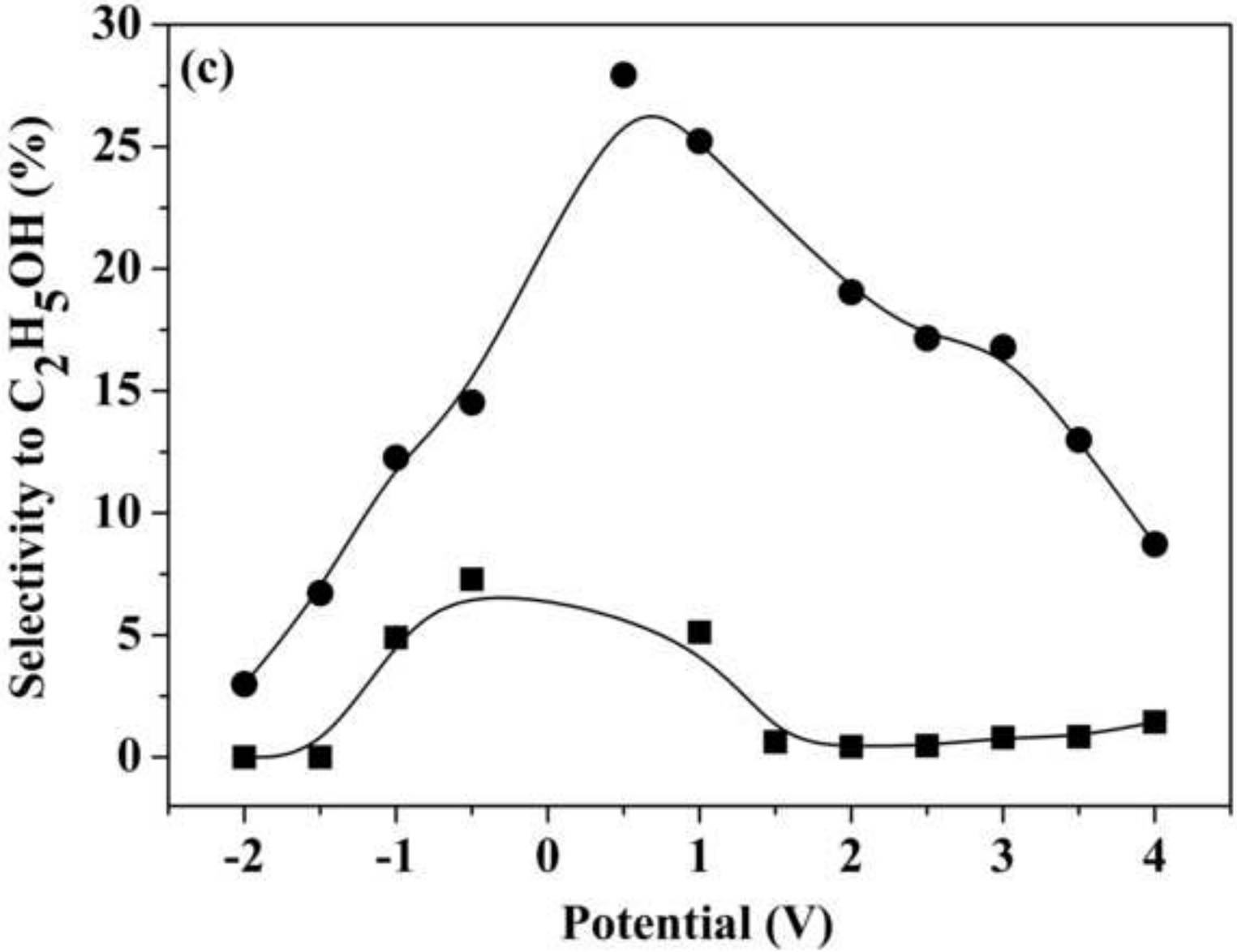

Fig.7(d).TIF
Click here to download high resolution image

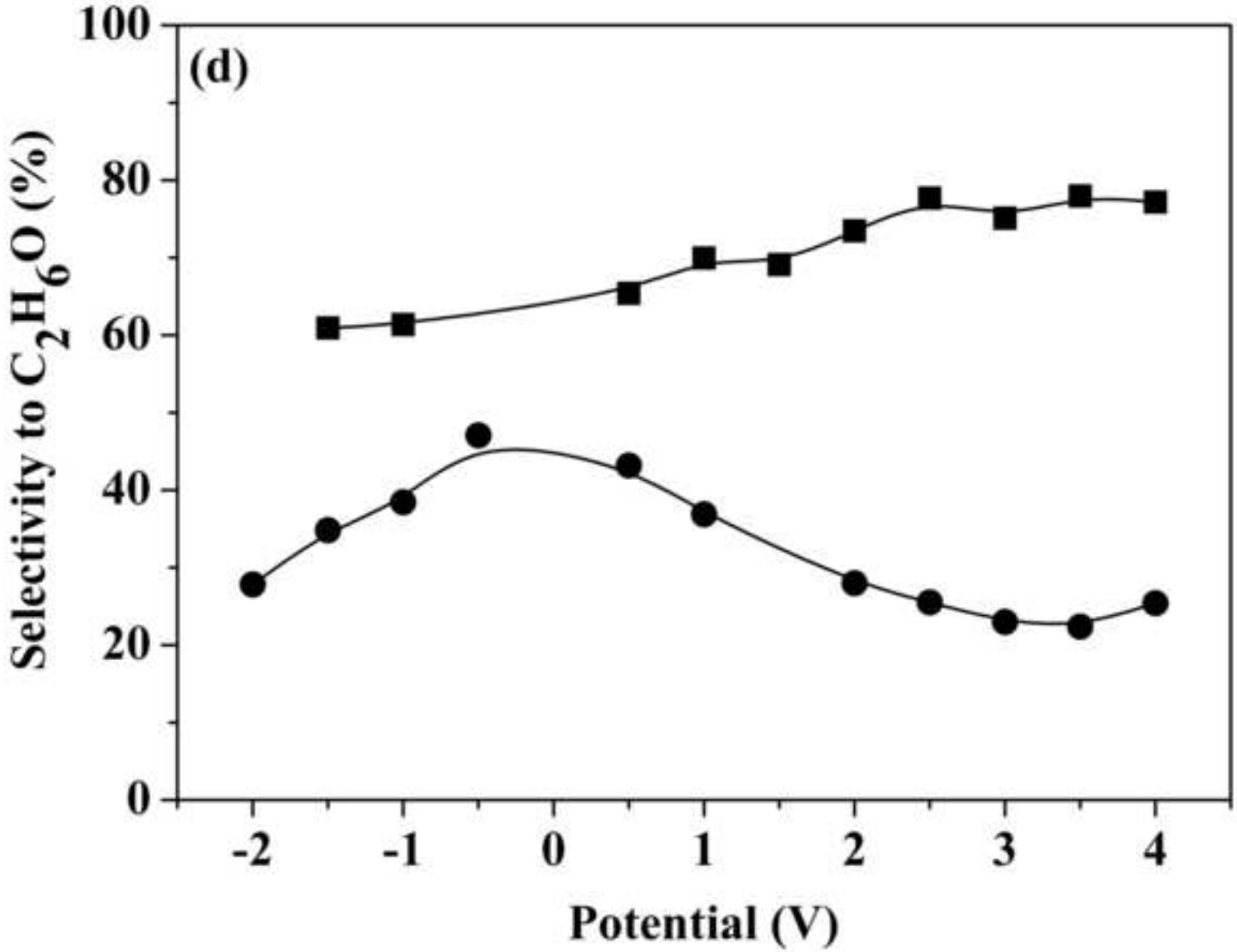

Fig.8.TIF
Click here to download high resolution image

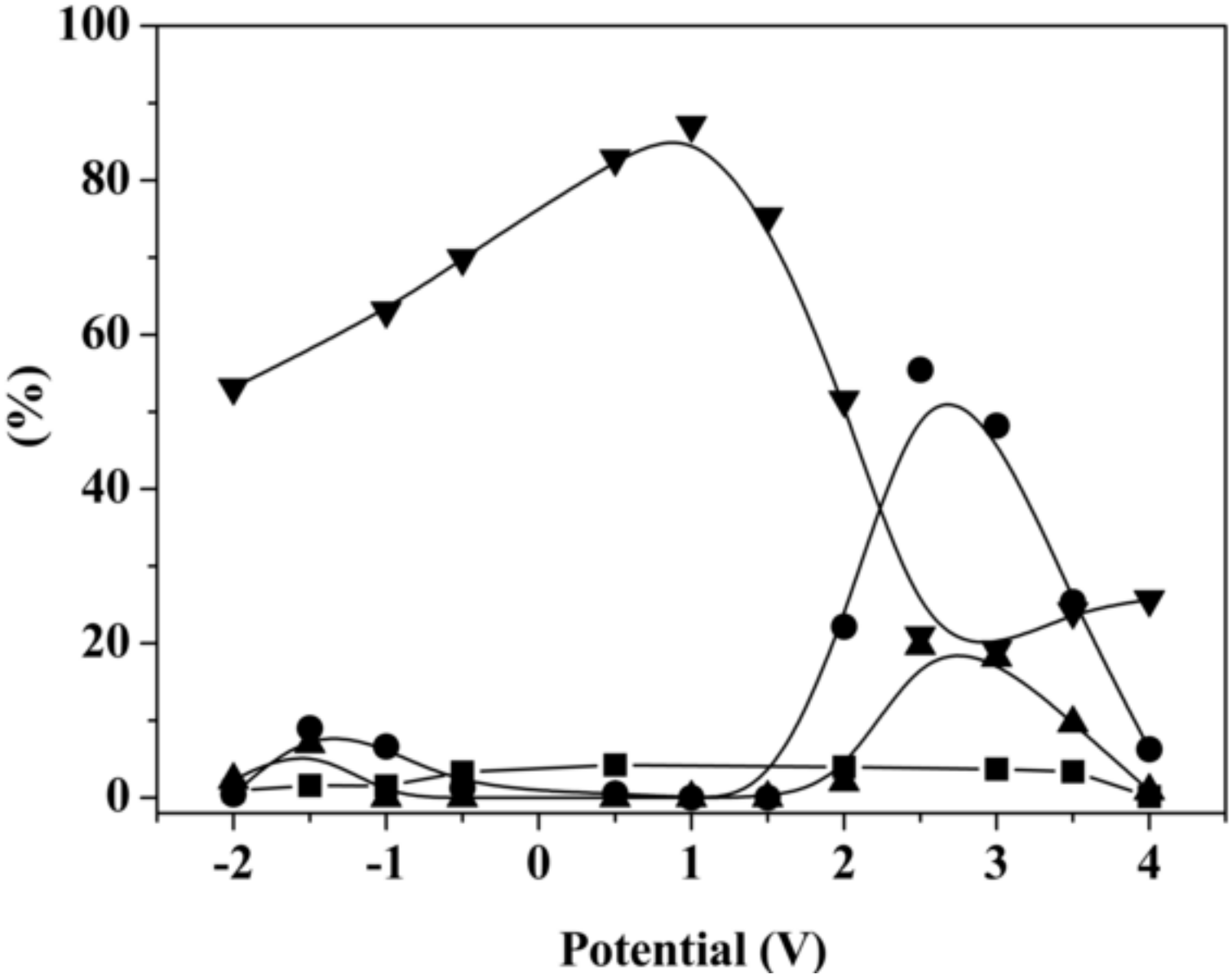

Fig.9.TIF
Click here to download high resolution image

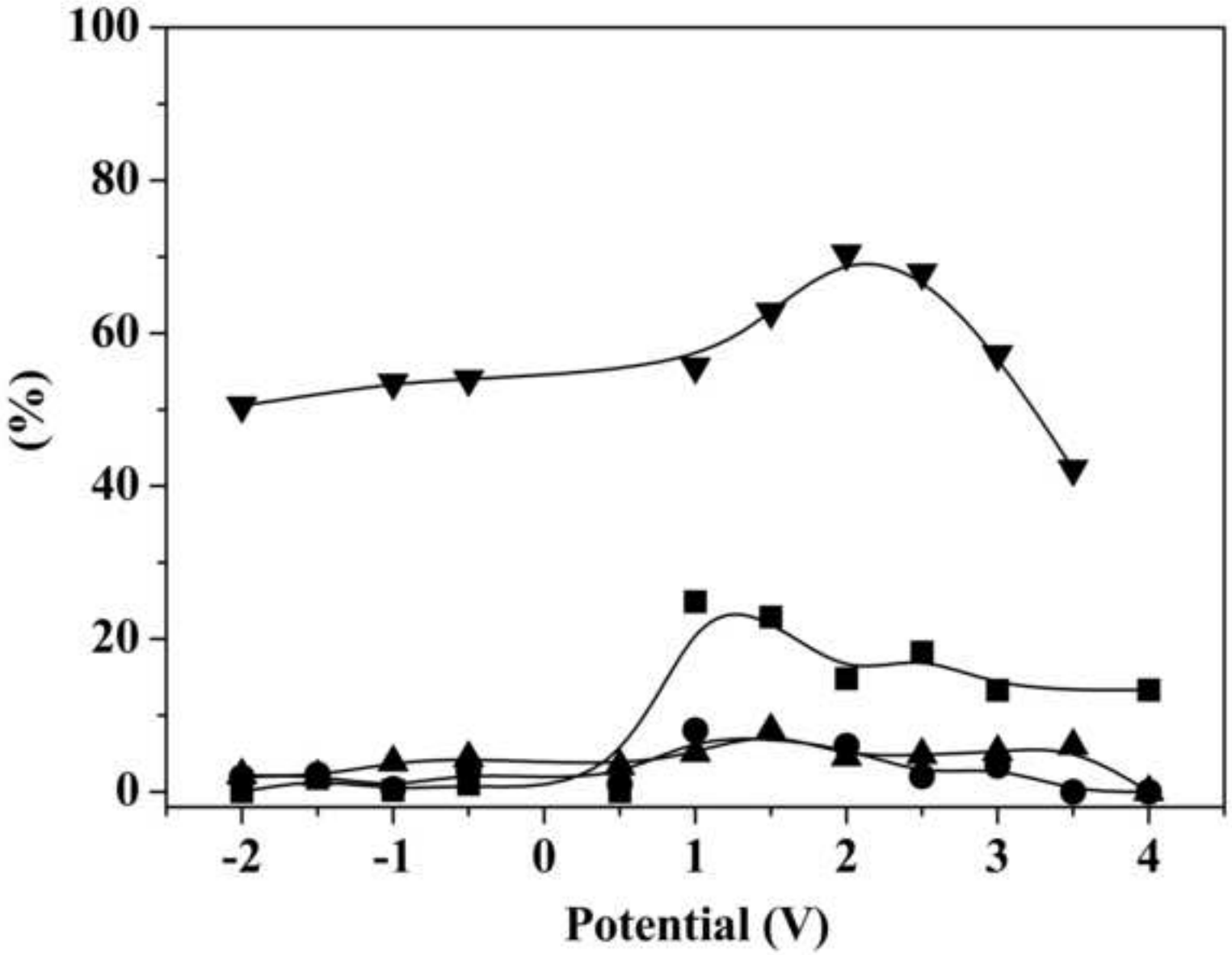

Fig.10(a).TIF
Click here to download high resolution image

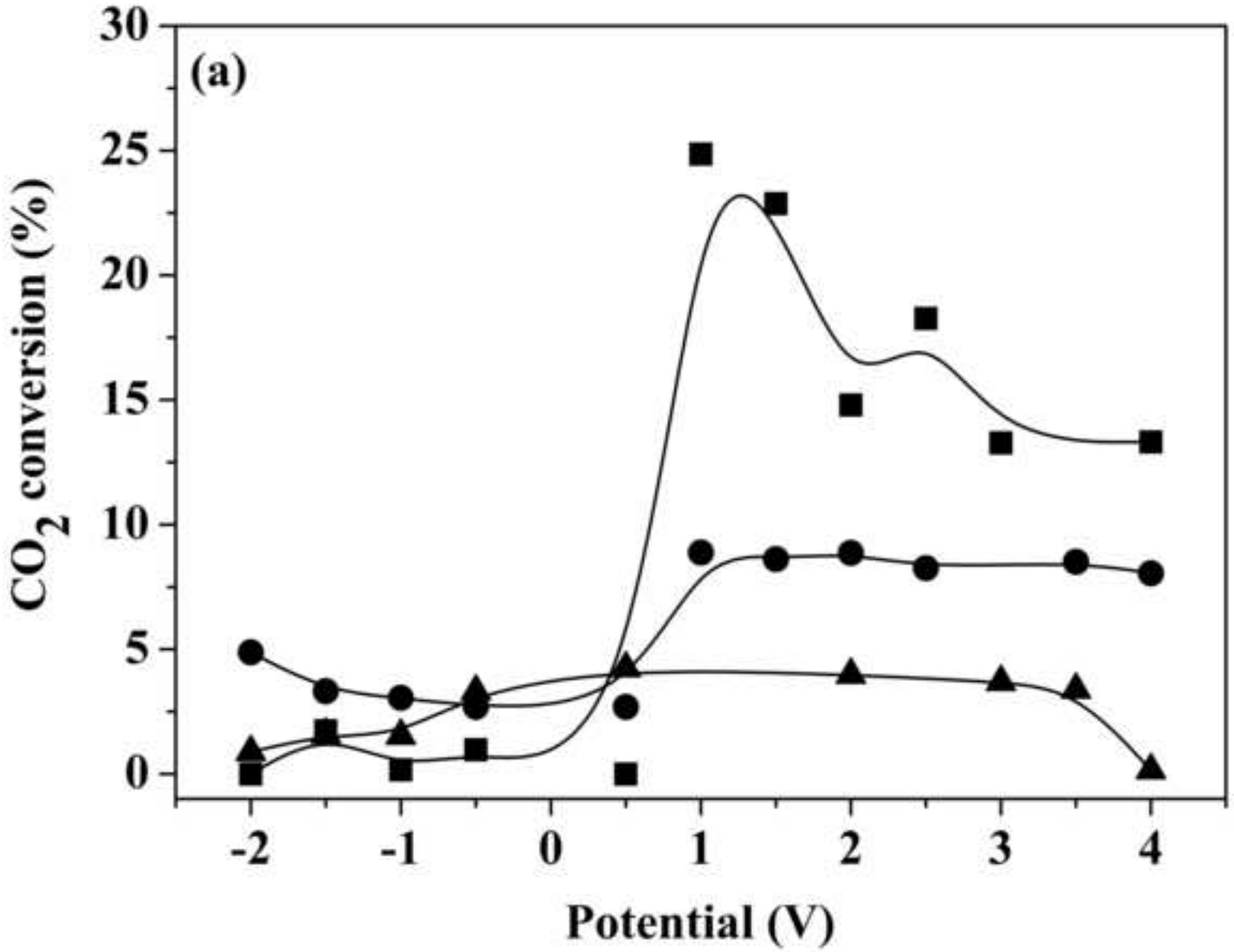

Fig.10(b).TIF
Click here to download high resolution image

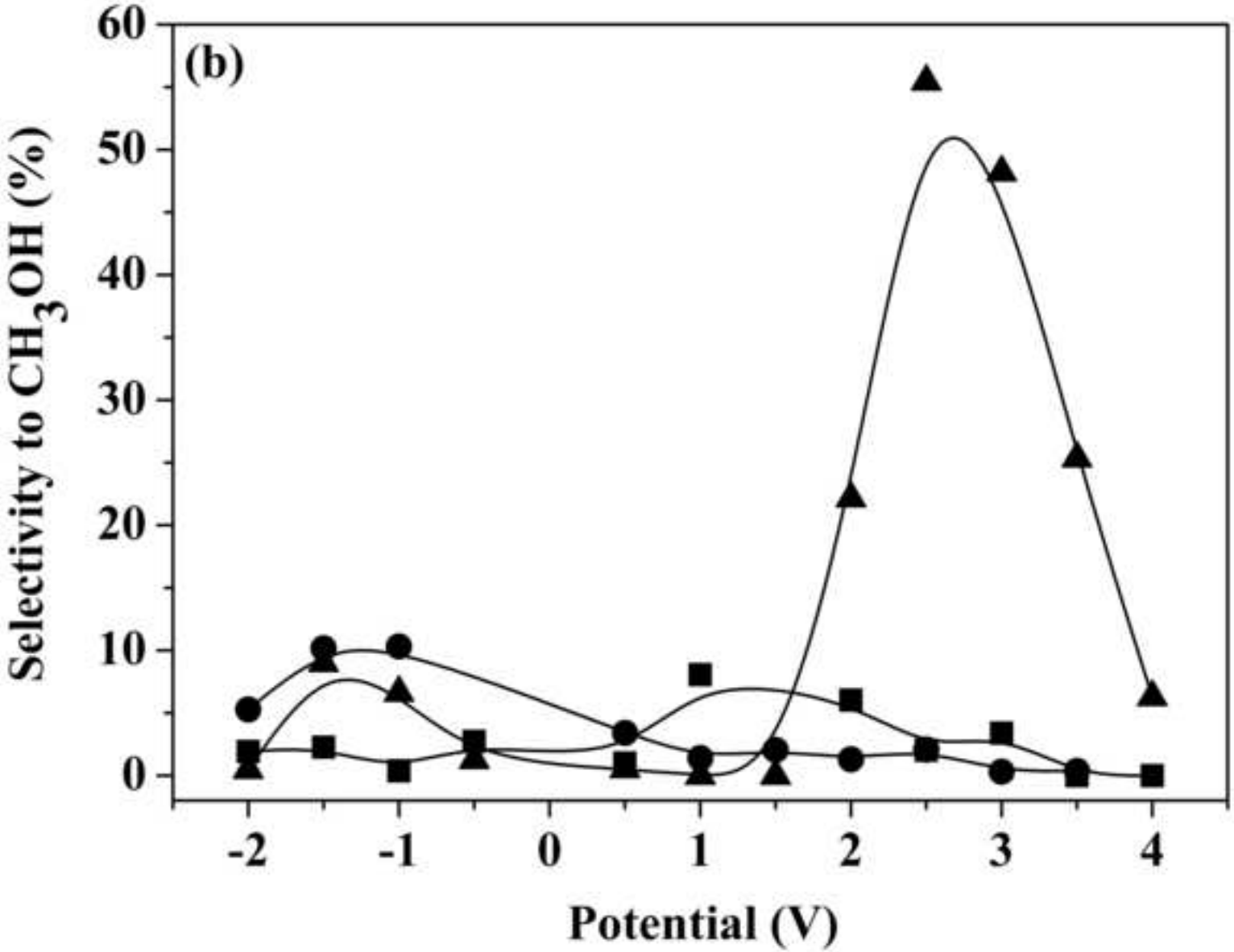

Fig.10(c).TIF
Click here to download high resolution image

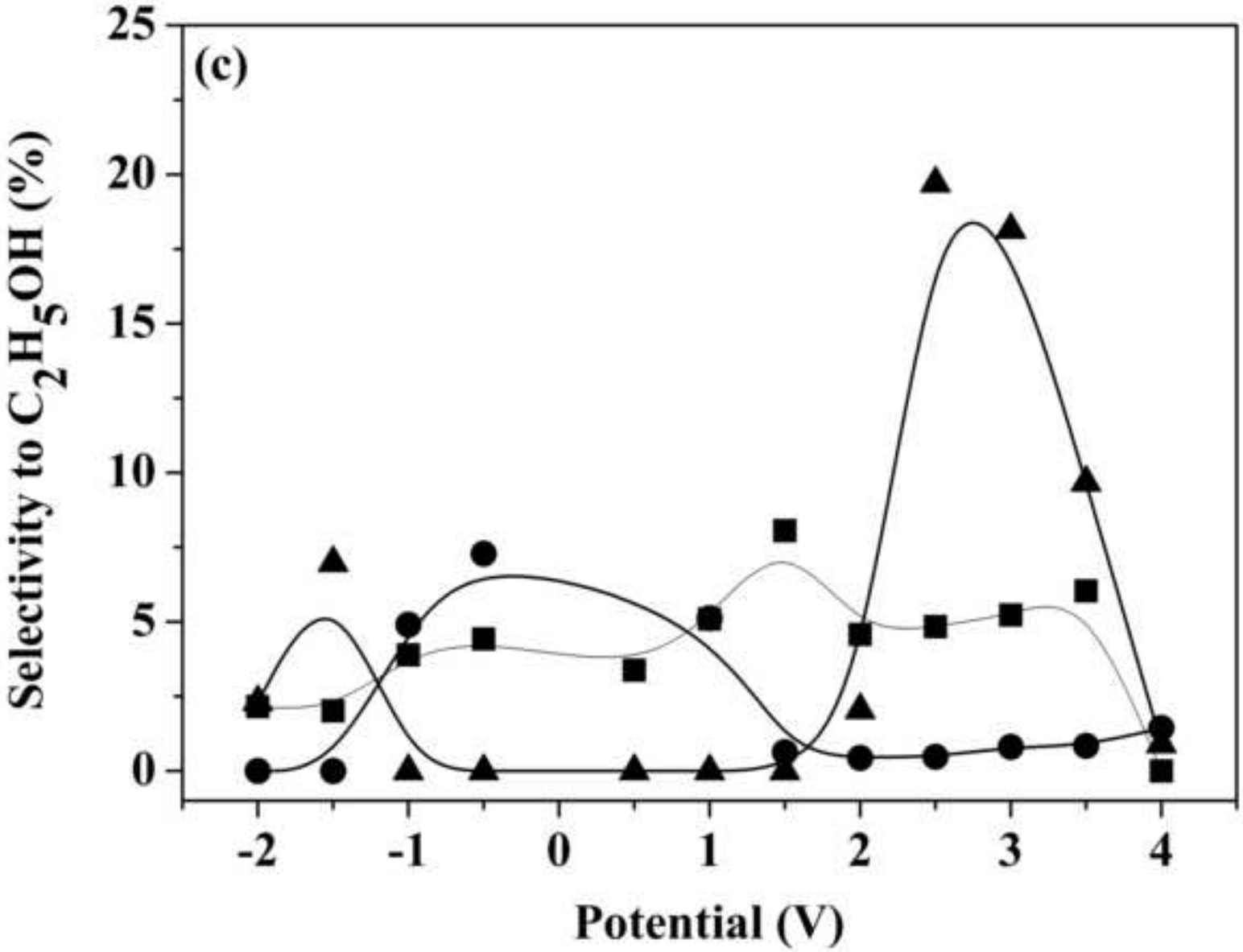

Fig.10(d).TIF
Click here to download high resolution image